Title

Cross-stream migration vs. anisotropic relaxation: Non-Boltzmann distributions in dissipative systems

Journal

AIChE Journal, 60(4)

ISSN

0001-1541

Author

Squires, Todd M

Publication Date

2014-04-01

DOI

10.1002/aic.14408

Peer reviewed

Cross-Stream Migration vs. Anisotropic Relaxation: Non-Boltzmann Distributions in Dissipative Systems

Todd M. Squires
Dept. of Chemical Engineering, University of California, Santa Barbara, CA 93106

DOI 10.1002/aic.14408
Published online in Wiley Online Library (wileyonlinelibrary.com)

Polymers and Brownian rods have been predicted and observed to migrate across streamlines in flowing systems, potentially impacting rheological measurements, material processing, and microfluidic systems. In particular, gradients in cross-stream diffusivity give rise to concentration gradients across streamlines, in direct contrast with naive expectations from equilibrium statistical mechanics. Here, we provide a simple, physicially intuitive understanding for the subtle mechanisms that underlie this counter-intuitive effect. Specifically, we identify three minimal ingredients: (1) the cross-stream diffusivity of the solute must depend on its internal degrees of freedom, (2) internal degrees of freedom must be driven nonconservatively in a position-dependent manner, and (3) a mechanism must exist for the concentration to relax to a steady state spatial proflie. Significantly, we argue that the inhomogeneous steady-state distributions that have been observed do not result from directed cross-stream migration. In fact, we show that no migration occurs in systems without spatial relaxation. Rather, concentration gradients are established due to anisotropic rates of spatial relaxation, and the lack of directed cross-stream migration that would be found in a conservative system. We demonstrate with simple model systems analogous to Brownian rods, externally triggerable two-state molecules, and in externally imposed temperature or solute gradients, which affect steady concentration profiles beyond what would be expected from thermophoresis or diffusiophoresis. Our results have implications for separation strategies and for various microfluidic and processing flows. © 2014 American Institute of Chemical Engineers *AIChE J*, 00: 000–000, 2014
Keywords: fluid mechanics, suspensions, rheology, transport

Background and Introduction

Understanding the behavior of small particles and macromolecules in suspension has long played a central role in fundamental and applied science. In particular, many techniques and technologies assume solute to remain homogeneously distributed. However, flows may drive unexpected concentration gradients, with deleterious effect. For example, polymer depletion layers near rheometer walls give an effective slip that causes material mischaracterization. Material processing flows can cause inhomogeneous particle distributions that degrade the finished product quality. Many sensing and detecting systems in microfluidics and biotechnology involve flowing solutions of target molecules that bind to wall- or bead-bound receptors.[1] If fluid flows along receptor-coated walls cause target molecules to migrate perpendicular to the walls, sensing rates will differ between stationary and flowing solutions. Hydrodynamic chromatographic separations are based on the relative amounts of time spent by particles of different sizes on streamlines of different speeds; unexpected mechanisms that influence particulate distribution will affect the resulting separation.

In addition to their applied importance, these issues raise questions that are deceptively simple to pose, yet whose resolution involves the subtle interplay of various fluid mechanical, statistical mechanical, and thermodynamical phenomena. When does intuition from equilibrium statistical mechanics carry over to flowing systems? For example, solutions of otherwise homogeneous polymers flowing through straight channels or cylinders have been observed to develop inhomogeneous concentration profiles, with concentration gradients perpendicular to fluid streamlines that are attributed to gradients in cross-stream diffusivity.[2–14] Such systems are steady in the Lagrangian sense—material elements moving along streamlines experience a temporarily steady environment—and no forces are exerted in directions across streamlines. One might naively hope that results from equilibrium statistical mechanics will apply, namely, a local concentration distribution that follows the Boltzmann distribution, with no dependence on kinetic parameters like viscosity and diffusivity. In many cases, such equilibrium expectations are recovered. Nonetheless, gradients in cross-stream diffusivity in even dilute solutions of flowing polymers give rise to non-Boltzmann distributions, despite the lack of a clear driving force that establishes them.

Although the dissipative nature of flowing systems gives cover for the failure of equilibrium theories, it leaves no simple means of discerning the physical mechanisms behind "cross-stream migration," nor does it provide any context to clearly distinguish flowing systems for which the Boltzmann distribution does indeed hold from those in which cross-stream inhomogeneities develop. In this work, we examine

Correspondence concerning this article should be addressed to T. M. Squires at squires@engineering.ucsb.edu.

dissipative systems that establish cross-stream concentration gradients, distill out the essential ingredients, and elucidate the mechanism by which they do so. In the spirit of using bead-spring models of varying complexity to capture the qualitative (and even quantitative) mechanistic phenomena for polymeric liquids,[15] we analyze simple model systems to elucidate phenomena that arise in systems that are more complicated mathematically and physically. In particular, we pose a series of paradigmatic model problems that are mathematically simpler than those that have been analyzed thus far. In so doing, we clearly identify three ingredients that are necessary and sufficient to give rise to this counter-intuitive phenomenon, and identify a clear, mechanistic picture by which these steady-state inhomogeneities develop. In fact, we demonstrate that the eventual concentration gradients arise not due to any directed cross-stream migration, as might be expected, but rather due to anisotropic relaxation. Perhaps ironically, it is the lack of directed, cross-stream migration that gives rise to cross-stream gradients. After all, anisotropic relaxation exists in equilibrium systems as well, wherein the Boltzmann distributions reflect the mutual cancelation between directed, cross-stream migration and anisotropic relaxation.

These insights allow us to propose a variety of new systems in which we predict analogous "gradient-relaxation drift," including colloidal and macromolecular (e.g., polymeric or protein) systems. Additionally, we will discuss this phenomenon in the context of thermophoresis and other solution gradients, and demonstrate that concentration gradients due to anisotrophic relaxation will arise in addition to any thermophoretic or multicomponent effects.

We begin by discussing what can be expected from suspended species in equilibrium systems. Because inertia is typically negligible in liquid solutions, particulate behavior is governed statistically by the Smoluchowski equation

$$\frac{\partial P}{\partial t} = -\nabla \cdot \mathbf{j} = \nabla \cdot \{\mathbf{D}(\mathbf{r})\nabla P + \mathbf{b}(\mathbf{r})\nabla\phi(\mathbf{r})P\} \tag{1}$$

Here $P(\mathbf{r},t)$ is the probability of finding the particle at $\mathbf{r}$ at time t, $\mathbf{j}$ is the probability flux, $\phi(\mathbf{r})$ is the potential energy (e.g., gravitational, electrostatic, or magnetic) for a particle located at $\mathbf{r}$, and the diffusivity and mobility tensors $\mathbf{D}(\mathbf{r})=k_\mathrm{B}T\mathbf{b}(\mathbf{r})$ are related via the fluctuation-dissipation theorem. In equilibrium, Eq. 1 is solved for arbitrary $\mathbf{D}(\mathbf{r})$ simply by the Boltzmann distribution

$$P_\mathrm{B}(\mathbf{r}) = P_0 e^{-\phi(\mathbf{r})/k_\mathrm{B}T} \tag{2}$$

Notably, no kinetic properties (viscosity, diffusivity, mobility) appear in the equilibrium distribution.

In flowing systems, the probability flux $\mathbf{j}$ is modified to include advection with the local fluid via

$$\mathbf{j}_a = \mathbf{u}(\mathbf{r})P \tag{3}$$

to give an advection–diffusion equation

$$\frac{\partial P}{\partial t} = \nabla \cdot \{\mathbf{D}(\mathbf{r})\nabla P + \mathbf{b}(\mathbf{r})\nabla\phi(\mathbf{r})P\} - \mathbf{u}(\mathbf{r}) \cdot \nabla P \tag{4}$$

In many cases of microfluidic, scientific, and industrial importance, flows occur along channels or walls and are, thus, perpendicular to confining forces ($\mathbf{u} \cdot \nabla\phi = 0$). One might expect the Boltzmann distribution (2) to thus hold, as

$$\mathbf{u}(\mathbf{r}) \cdot \nabla P_\mathrm{B}(\mathbf{r}) = -\frac{P_\mathrm{B}(\mathbf{r})}{k_\mathrm{B}T}\mathbf{u} \cdot \nabla\phi = 0 \tag{5}$$

even though the system is not in equilibrium.

Although the Boltzmann distribution is indeed often observed in flowing systems, curious exceptions can be observed even in homogeneous systems with $\mathbf{u} \cdot \nabla\phi = 0$ everywhere. One might suspect that suspended particles migrate across streamlines due to deterministic, hydrodynamic interactions with channel walls; however, general and powerful symmetry arguments based on the reversibility of Stokes flow[16–18] do not allow such cross-stream migration for rigid particles in the low-Reynolds number limit of interest here.

Additional physics are required to break this reversibility and drive particles across streamlines. For example, inertia can induce drift away from walls,[19,20] and can be exploited to manipulate particles and cells in "intertial microfluidics."[21] Many-body collisions in driven colloidal suspensions give rise to "shear-enhanced migration" toward regions of low shear,[22] and induce chaos that breaks irreversibility even in deterministic, non-Brownian suspensions.[23] Deformable bodies in flow (e.g., red blood cells,[24] emulsion drops,[25] and polymers[2–4,6,10–12]) migrate away from walls via a well-known hydrodynamic force-dipole mechanism.[25]

Less easily explained, however, are the low polymer concentrations observed in the center of channel flows,[5,6,8,10,11] despite the irrelevance of many-body effects, the lack of nearby walls, and the absence of flows or forces that would drive a cross-stream migration. Early theories appealed to equilibrium statistical mechanics, and argued that systems seek less deformed states to maximize entropy (see, e.g., Ref. 2 for a review). However, dissipative systems need not obey even the basic principles of equilibrium statistical mechanics. Here, by contrast, deformable bodies move to maximize deformation.

Two model systems have been studied explicitly to address these flowing polymer systems: Brownian rods[3,4] and bead-chain polymers[6,8,11] in parabolic flow between channel walls. Through simulations and multiple-timescale analyses, this subtle "cross-stream migration" has been argued to result from a diffusivity that depends on rod/polymer configuration, and configurations that are driven out of equilibrium by the (position-dependent) flow.

Basic System

For guidance, we turn to a minimal system that gives rise to non-Boltzmann profiles under steady-state flows. For mathematical simplicity, we consider a particle whose state $P(q,y,t)$ can be described by two Cartesian co-ordinates: y as a physical location and q as a "configuration" (Figure 1). The translational y-diffusivity D_{yy} depends on configuration q, which is driven in a nonconservative, y-dependent manner (i.e., with a convective flux $u_q(y)$ in configuration space), to give a Smoluchowski equation

$$\frac{\partial P}{\partial t} = \frac{\partial}{\partial q}\left(D_{qq}\frac{\partial P}{\partial q} - u_q(y)P\right) + \frac{\partial}{\partial y}\left(D_{yy}(q)\frac{\partial P}{\partial y}\right) \tag{6}$$

More generally, some conservative force ϕ (e.g., an external magnetic field) might affect the configuration, in which case

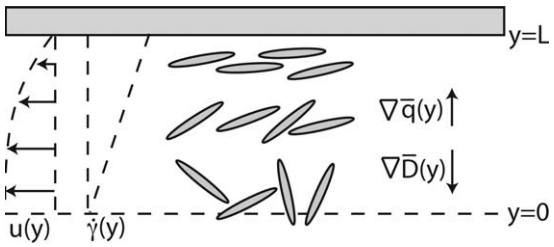

Figure 1. Model system for cross-stream concentration gradient formation.

A solute flows at cross-stream position y along a channel, and possesses a configuration or internal degree of freedom, denoted by a Cartesian variable q (which is here depicted as rod orientation.) The cross-stream diffusivity $D_{yy}(q)$ is taken to depend upon configuration (just as rod diffusivity depends upon orientation), and the configuration is driven in a nonconservative, position-dependent way (here depicted as a shear-rate gradient that orients the rod to a varying amount.)

$$\frac{\partial P}{\partial t}=\frac{\partial}{\partial q}\left(D_{qq}\frac{\partial P}{\partial q}-\alpha(y)P\right)+\frac{\partial}{\partial y}\left(D_{yy}(q)\frac{\partial P}{\partial y}\right) \tag{7}$$

where

$$\alpha(y)=u_q(y)-\frac{D_{qq}}{k_BT}\frac{\partial \phi}{\partial q} \tag{8}$$

We have deliberately stripped our model system of as many mathematical complications as possible, for clarity and ease of presentation. One analogous physical representation of this system would be a Brownian rod flowing in a Poiseuille flow between straight channel walls (Figure 1). The location of the rod within the channel is given by y, and the rod's orientation angle (described in the full, physical system by one or two rotation angles) is simplified here to a Cartesian variable q in our model system. The translational (cross-stream) diffusivity D_{yy} of the rod at each instant depends on its orientation q, as diffusivity parallel to the axis of an infinitely thin rod is double that perpendicular to the axis (e.g., Ref. 17). Finally, any local shear rate changes the average alignment of the rod [introducing a peak to an orientation distribution function $P(\theta,\phi)$, here simplified as changing the "q" distribution function $P(q)$] in a spatially nonhomogeneous way: stronger shear rates (near walls) shift the peak in conformation space to greater average orientations. A different realization of this basic system would be a (deformable) polymer in flow, whose configuration variable "q" could be multidimensional, depending on the level of detail it was modeled.

We briefly adapt the multiple-scales analysis from Ref. 3 to the present system (Eq. 7). If gradients in y are small and configurations q relax quickly, then a quasisteady distribution in q is achieved at each position y

$$P(q,y,\tau)\sim A(y,\tau)\exp\left(\frac{u_q(y)q}{D_{qq}}-\frac{\phi(q)}{k_BT}\right) \tag{9}$$

where the time scale τ over which the local concentration A evolves is long compared with the relaxation time for configurations. A steady distribution $P_s(q,y)$ is achieved, when there is no net flux in the y-direction

$$\int D_{yy}(q)\frac{\partial P_s(q,y)}{\partial y}dq=0 \tag{10}$$

where we have integrated over all possible configurations q. This no-flux condition

$$\frac{\partial}{\partial y}\left[A_s(y)\int_{-\infty}^{\infty}D_{yy}(q)\exp\left(\frac{u_q(y)q}{D_{qq}}-\frac{\phi(q)}{k_BT}\right)dq\right]=0 \tag{11}$$

can be directly integrated via

$$A_s(y)\int_{-\infty}^{\infty}D_{yy}(q)\exp\left(\frac{u_q(y)q}{D_{qq}}-\frac{\phi(q)}{k_BT}\right)dq=C_0 \tag{12}$$

to give an explicit form for the prefactor A_s

$$A_s(y)=C_0\left(\int_{-\infty}^{\infty}D_{yy}(q)\exp\left(\frac{u_q(y)q}{D_{qq}}-\frac{\phi(q)}{k_BT}\right)dq\right)^{-1} \tag{13}$$

The steady-state concentration $C_s(y)$ is thus inhomogeneous and given by

$$C_s(y)=\int P_s(q,y)dq=\frac{C_0\int e^{\left(\frac{u_q(y)q}{D_{qq}}-\frac{\phi(q)}{k_BT}\right)}dq}{\int D_{yy}(q)e^{\left(\frac{u_q(y)q}{D_{qq}}-\frac{\phi(q)}{k_BT}\right)}dq} \tag{14}$$

Analogous integrals for the specific system of Brownian rods in Poiseuille flow are given in Ref. 3.

Significantly, neither forces nor advective flows exist that drive particles across streamlines (i.e., in the y-direction). Nonetheless, a nonuniform (non-Boltzmann) concentration profile is attained, wherein concentrations are higher where cross-stream diffusivities are lower. This would appear to require two key features: a configuration-dependent translational diffusivity $D_{yy}(q)$, and configurations that are driven by a nonconservative "advection" $u_q(y)$. If D_{yy} were independent of configuration q, it could be taken outside the integral in (13) and (14) would give a constant concentration $C_s=C_0/D_0$. If the "configuration advection" u_q did not depend on position y, the right-hand side of (14) would simply be constant. Finally, in a conservative system, the configuration flux u_q would be derivable from a scalar potential

$$u_q^{\text{cons}}(y)=-\frac{\partial \Phi}{\partial q} \tag{15}$$

which would, in turn, introduce a positional advection

$$u_y^{\text{cons}}=-\frac{\partial \Phi}{\partial y}\sim q\frac{\partial u_q}{\partial y} \tag{16}$$

whereupon (6) would simply give a Boltzmann distribution for C_s.

How are these non-Boltzmann concentration profiles established? One might naturally expect that the local flow induces a directed, cross-stream drift. We now demonstrate, however, that no average drift occurs in an unbounded system. The Smoluchowski equation (6) represents conservation of probability

$$\dot{P}=-\nabla\cdot\mathbf{j} \tag{17}$$

where $\mathbf{j}$ consists of probability fluxes, both in configuration

$$j^q=-D_{qq}\frac{\partial P}{\partial q}+u(y)P-\frac{D_{qq}}{k_BT}\frac{\partial \phi}{\partial q}P \tag{18}$$

and position

$$j^y=-D_{yy}(q)\frac{\partial P}{\partial y} \tag{19}$$

Multiplying the Smoluchowski equation (17) by y, and integrating over q and y gives an evolution equation for $\langle y \rangle$

$$\frac{\partial \langle y \rangle}{\partial t} = -\int y \left(\int \frac{\partial j^q}{\partial q} dq \right) dy - \int \left(\int y \frac{\partial j^y}{\partial y} dy \right) dq \tag{20}$$

The first term vanishes identically upon integration because $j^q = 0$ at infinity, and the second may be integrated by parts to yield

$$\int \int j^y dy dq = \int \int D_{yy}(q) \frac{\partial P}{\partial y} dy dq \tag{21}$$

which direct integration gives

$$\frac{\partial \langle y \rangle}{\partial t} = -\int D_{yy}(q) P \Big|_{y=-\infty}^{y=\infty} dq \tag{22}$$

Since $P(y = \pm\infty) \equiv 0$ at any finite time, the cross-stream drift is given precisely by

$$\frac{\partial \langle y \rangle}{\partial t} \equiv 0 \tag{23}$$

We are now faced with an apparent contradiction: this system evolves from an initial Boltzmann concentration to a non-Boltzmann distribution (14) under a nonconservative configuration "flux." Although one might expect this to result from a directed, cross-stream migration, we have shown that there is identically zero drift in this system. How can these two observations be reconciled?

We now argue that anisotropies in the way that concentration profiles relax to steady state, rather than any net cross-stream drift velocity, are responsible for the eventual non-Boltzmann steady state. Arguments based on the steady state obscure the dynamics that must occur to establish that steady state. The lack of any mean drift (Eq. 23) in the simplest model system (a polymer or rod flowing within a channel[3,4,6,11,12]), arises because no mechanism exists for concentration profiles to relax to a steady state—rather, the profiles can simply spread without bound. Steady state is never achieved in the unbounded system, as the spatial relaxation time is infinite.

Particles flowing between two no-flux channel walls ($y = \pm L$), however, experience no confining force until they encounter the wall, which exerts whatever force is required to maintain the no-flux condition. Repeating the above argument for systems bounded by no-flux walls at $\pm L$ modifies (22) to give

$$\frac{\partial \langle y \rangle}{\partial t} = -\int D_{yy}(q)[P(q, L) - P(q, -L)] dq \tag{24}$$

which is not generally zero. The position-dependent "configuration advection" gives a different configuration distribution $P(q, \pm L)$ at the top and bottom surfaces. The no-flux boundary effectively takes those particles that would have diffused past $\pm L$ in an unconfined system, and injects them back in. It is the diffusivity difference between particles reinjected at the top ($y = L$) vs. those at the bottom ($y = -L$) that leads to the eventual cross-stream gradients. In other words, the particles themselves experience no net migration within the channel—as many fluctuate up as down, and the ensemble-averaged position does not drift—until particles experience a confining force that drives their positional relaxation. The response to this confining force depends on the local mobility $b_{yy} = D_{yy}/k_B T$ of the solute: those particles that reach the upper wall (where D_{yy} is lower) take longer to return than those that reach the channel center (where D_{yy} is higher). Therefore, solute gradually accumulates in regions of low average diffusivity over time scales relevant for positional relaxation (here given by $\tau \sim L^2/D_{yy}$).

Conservative Systems

The same anisotropy in positional relaxation occurs in conservative systems, whenever spatial diffusivity D_{yy} depends on position y. How is it that equilibrium systems avoid non-Boltzmann concentrations? For guidance, we turn to the minimal conservative system, which has spatially varying diffusivity $D_{yy}(y)$ but no internal degrees of freedom q. Its Smoluchowski equation

$$\frac{\partial P}{\partial t} = \frac{\partial}{\partial y} \left(D(y) \frac{\partial P}{\partial y} \right) \tag{25}$$

when multiplied by y and integrated over all y, yields an evolution equation for the mean position

$$\frac{\partial \langle y \rangle}{\partial t} = -\int y \frac{\partial j^y}{\partial y} dy = y j^y \Big|_{-L}^{L} + \int j^y dy \tag{26}$$

The first term on the right vanishes because there is no flux from "outside"—whether at infinity or at a boundary. The second term involves a diffusive flux, which can be integrated by parts to give

$$\int D \frac{\partial P}{\partial y} dy = D(y) P(y) \Big|_{-L}^{L} - \int P(y) \frac{\partial D}{\partial y} dy \tag{27}$$

so that

$$\frac{\partial \langle y \rangle}{\partial t} = \int P(y) \frac{\partial D}{\partial y} dy - D(y) P(y) \Big|_{-L}^{L} \tag{28}$$

The $D(y)P(y)|_{-L}^{L}$ term is the precise analog of Eq. 24, describing the anisotropic "reinjection" of particles due to the confining forces imposed by the two walls, and drives a gradual accumulation of solute in regions of low diffusivity. The $\int P(y) \partial_y D dy$ term, however, has no analog in the systems described above. Any diffusivity that depends explicitly on position y drives a true cross-stream migratory velocity toward regions of greater diffusivity, as though the solute species were convected with velocity $\nabla \cdot \mathbf{D}$. Thus, even in an unbounded system ($L \to \infty$, in the absence of relaxation)—there is a nonzero solute drift up diffusivity gradients. In equilibrium, this drift is precisely counteracted by the anisotropic positional relaxation: a constant concentration $P(y) = P_0$, satisfying the Boltzmann distribution, clearly satisfies Eq. 28

$$\frac{\partial \langle y \rangle}{\partial t} = P_0 D(y) \Big|_{-L}^{L} - P_0[D(L) - D(-L)] \equiv 0 \tag{29}$$

By contrast, a spatial diffusivity D_{yy} that does not depend explicitly on position y, but rather on configuration q, which on average depends on position y, exhibits no $\nabla \cdot \mathbf{D}$ drift to cancel the anisotropic positional relaxation, giving rise to non-Boltzmann distributions as in Eq. 24.

It is perhaps ironic that the non-Boltzmann concentration gradients attained in steady-state flowing systems arise due to the absence of a cross-stream drift velocity. The hallmark of the phenomenon described here is that concentration gradients build only through anisotropic relaxation of the

concentration field. An ensemble of particles experiences zero net drift until the particle positions are forced to relax toward a steady state, at which point the cross-stream gradients in mobility and diffusivity cause positional relaxation from one end to occur more quickly than from the other.

Specific Model Calculations

Having laid the general framework for cross-stream gradient formation via anisotropic relaxation, we now demonstrate with explicit calculations of the dynamics of three paradigmatic model systems, each of which illustrates a different feature. The first involves a solute whose configuration q and position y are both confined by harmonic potential wells. The second involves a solute whose configuration q is harmonically confined, but whose position y is confined between two planar walls, and thus, which relaxes purely diffusively. Although the latter is the simplest and most direct analog of the flowing suspensions described initially, it is algebraically more cumbersome than the harmonic system. These two examples involve different relaxation mechanisms, in line with the general role for relaxation we have argued. A particular benefit of these two computations is that they elucidate the dynamic, transient processes by which cross-stream gradients arise. To generalize our picture beyond continuous degrees of freedom (like rotation), we examine a third model system with two discrete states, such as a protein or macromolecule that can be folded or unfolded. Finally, we examine particles in solutions with imposed gradients (e.g., thermal or solute), wherein "differential relaxation" drives steady-state concentration gradients in addition to those driven by thermophoretic or diffusiophoretic drift.

Doubly harmonic potential well

We begin with perhaps the simplest model system (Fig. 3) in which anisotropic relaxation gives rise to cross-stream gradients. Specifically, we consider a solute whose positional diffusivity $D_{YY}(Q)$ depends linearly on "configuration" Q via

$$D_{YY}(Q)=D_0(1+\epsilon Q) \tag{30}$$

where D_0 is a constant diffusivity. We assume this linear dependence for the sake of analytical tractibility and to illustrate the fundamental mechanism behind this phenomenon, rather than because it accurately describes a range of systems. Although rods[3,4] and near-spheres[26] have diffusivities with a mild $\mathcal{O}(1)$ dependence on orientation (at most a factor 2 for rods of infinite aspect ratio[17]), deformable solutes like polymers can stretch significantly to yield extremely large differences in diffusivities when subjected to different flows.

The solute sits in a doubly harmonic potential well that confines both position and configuration

$$\Phi(Q,Y)=k_BT\left(\frac{Q^2}{2L_q^2}+\frac{Y^2}{2L_y^2}\right) \tag{31}$$

so that spring constants in the Q- and Y-directions are

$$k_Q=\frac{k_BT}{L_Q^2},\quad k_Y=\frac{k_BT}{L_Y^2} \tag{32}$$

Finally, a nonconservative flux drives conformational changes in a position-dependent manner, via

$$u_Q=-\dot{\gamma}Y \tag{33}$$

Note, here that the capital variables Q, Y, and T represent dimensional quantities; later, nondimensionalized quantities will be represented by lower-case variables.

The Smoluchowski equation for this system is

$$\frac{\partial P}{\partial T}=-\frac{\partial j_Q}{\partial Q}-\frac{\partial j_Y}{\partial Y} \tag{34}$$

where

$$j_Q=-D_0\frac{\partial P}{\partial Q}-\dot{\gamma}YP-D_0\frac{QP}{L_q^2} \tag{35}$$

and

$$j_Y=-D_0(1+\epsilon Q)\left(-\frac{\partial P}{\partial Y}-\frac{YP}{L_Y^2}\right) \tag{36}$$

We take the particle to start at $Q_0=Y_0=0$ at $T=0$. Scaling lengths Q and Y by typical Q-excursions from the center of the well, L_Q, and time T by the Q-relaxation time back to the center of the well, L_Q^2/D_0, we obtain a nondimensionalized equation

$$\frac{\partial P}{\partial t}=P_{qq}+\alpha yP_q+(qP)_q+(1+\beta q)\left(P_{yy}+\tau^{-1}(yP)_y\right) \tag{37}$$

Here, the parameter α

$$\alpha=\frac{\dot{\gamma}L_q^2}{D_0}\ll 1 \tag{38}$$

is a dimensionless shear rate, and relates the time to diffusively explore "configuration space" (i.e., to diffusively explore the q-well) to the shear shear time $\dot{\gamma}^{-1}$. The parameter β

$$\beta=L_q\epsilon\ll 1 \tag{39}$$

relates the spatial extent of the configuration well to the length scale over which the diffusivity varies (ϵ^{-1}); and τ

$$\tau=\frac{L_y^2}{L_q^2}\gg 1 \tag{40}$$

gives the positional relaxation time scaled by the configurational relaxation time. We assume configurations relax much more quickly than position within the channel, so $\tau\gg 1$, and that the q-spring is much "stronger" than the y-spring, so that y-excursions are larger than q-excursions by $\mathcal{O}\left(\tau^{1/2}\right)$.

It will prove convenient to rearrange the Smoluchowski equation as

$$\mathcal{L}_0P=\alpha yP_q+\beta qP_{yy}+\beta\tau^{-1}q(yP)_y \tag{41}$$

where

$$\mathcal{L}_0P\equiv\frac{\partial P}{\partial t}-P_{qq}-(qP)_q-P_{yy}-\tau^{-1}(yP)_y \tag{42}$$

gives the dynamics of the "unforced" system, wherein a particle diffuses within a doubly harmonic potential well.

Before launching into a full, propagator-based treatment, the steady problem can be readily be solved using a perturbation expansion

$$P^s(q,y)=P_0^s+\alpha P_\alpha^s+\beta P_\beta^s+\alpha\beta\left[P_{\alpha\beta}^s+P_{\beta\alpha}^s\right] \tag{43}$$

where

$$P_\alpha^s = \mathcal{L}_0^{-1}\left(y\frac{\partial P_0^s}{\partial q}\right) \tag{44}$$

$$P_{\alpha\beta}^s = \mathcal{L}_0^{-1}\left[q\frac{\partial^2 P_\alpha^s}{\partial y^2} + \frac{q}{\tau}\frac{\partial}{\partial y}\left(yP_\alpha^s\right)\right] \tag{45}$$

and so on. By way of notation, $P_{\alpha\beta}$ is the solution arising from the "source" terms $\beta q P_{\alpha,yy}$, $P_{\beta\alpha}$ arises from $\alpha y P_{\beta,q}$ and so on. The steady distributions can be shown to be given by

$$P_0^s(q,y) = \frac{e^{-q^2/2 - y^2/(2\tau)}}{2\pi\tau^{1/2}} \tag{46}$$

$$P_\alpha^s(q,y) = -\tau^{1/2} q y \frac{e^{-q^2/2 - y^2/(2\tau)}}{2\pi(1+\tau)} \tag{47}$$

$$P_\beta^s(q,y) = 0 \tag{48}$$

$$P_{\alpha\beta}^s(q,y) = \frac{\tau^{1/2}(2\tau+q^2)y}{(1+3\tau+2\tau^2)}\frac{e^{-q^2/2 - y^2/(2\tau)}}{2\pi} \tag{49}$$

$$P_{\beta\alpha}^s(q,y) = 0 \tag{50}$$

The ensemble-averaged displacement $\bar{y}^s$, computed using (43) in

$$\bar{y}^s = \int_{-\infty}^{\infty}\int_{-\infty}^{\infty} y P^s(q,y)\,dq\,dy \tag{51}$$

is zero for all terms smaller than $\mathcal{O}(\alpha\beta)$, with the first nonzero contribution to $\bar{y}^s$

$$\bar{y}^s = \alpha\beta\frac{\tau^2}{1+\tau} \tag{52}$$

arising exclusively from $P_{\alpha\beta}$, which represents particles whose configurations are first driven by a position-dependent advection (giving αP_α^s), and whose positions then relax back to the center anisotropically (introducing τ), due to the configuration-dependent diffusivity/mobility (giving β). This is the mechanism indicated in Figure 2. By contrast, $P_{\beta\alpha}^s$ — which reflects contributions from particles that first diffuse anisotropically, then experience conformation advection—is actually zero, and does not contribute to $\bar{y}^s$.

Because two-dimensional (2-D) diffusion in a harmonic well

$$\mathcal{L}_0 P = 0 \tag{53}$$

subject to initial conditions

$$P(q,y,0) = \delta(q-q_0)\delta(y-y_0) \tag{54}$$

can be solved exactly,[27] and because the forcing terms on the right-hand side of Eq. 41 are all small, we can treat this system perturbatively. The leading-order behavior is described simply by the unperturbed propagator $\mathcal{L}_0$ for a particle diffusing in a 2-D harmonic well, with the right-hand terms acting as "source" terms much as weak scatters act as source terms for scattering. A significant benefit to this approach is that it elucidates the dynamic mechanism that gives rise to the gradients we seek to understand, as the order in which the processes occur (advection, relaxation, etc.) is accounted for naturally.

To examine the full, time-dependent behavior of this system, we pose an expansion of the form

$$P(q,y,t) = P_0 + \alpha P_\alpha + \beta P_\beta + \alpha\beta(P_{\alpha\beta} + P_{\beta\alpha}) + \ldots \tag{55}$$

where the "free" propagator P_0 relates the probability that a particle starting at $\{q_0, y_0\}$ within a doubly harmonic potential at time t_0 will be located at $\{q, y\}$ at time t, and is given by[27]

$$P_0(q,y,t;q_0,y_0,t_0) = f(q,q_0,t,t_0)\,g(y,y_0,t,t_0) \tag{56}$$

where

$$f(q,q_0,t,t_0) = \frac{\exp\left(-\frac{(q-q_0 e^{-(t-t_0)})^2}{2(1-e^{-2(t-t_0)})}\right)}{\sqrt{2\pi}\left(1-e^{-2(t-t_0)}\right)^{1/2}} \tag{57}$$

$$g(y,y_0,t,t_0) = \frac{\exp\left(-\frac{(y-y_0 e^{-(t-t_0)/\tau})^2}{2\tau(1-e^{-2(t-t_0)/\tau})}\right)}{\sqrt{2\pi}\tau^{1/2}\left(1-e^{-2(t-t_0)/\tau}\right)^{1/2}} \tag{58}$$

We now sketch the perturbation calculation; details are given in Appendix B. We take the particle as initially being located at the origin at time $t = 0$. At any later time t', the particle has a probability $P_0(q',y',t',0,0,0)$ of being located at $\{q',y'\}$. Therefore, at time t' the "advective" perturbation effectively gives rise to sources and sinks according to $\alpha y' \partial P_0/\partial q'$, each of which then propagates in time via $P_0(q, y, t; q', y', t')$ to contribute to the resulting probability of being at $\{q,y\}$ at time t. Since advective perturbations occur at any time t' between zero and t, the full advective contribution is found by integrating over all times from zero to t

$$P_\alpha(q,y,t) = \mathcal{L}_0^{-1} y\frac{\partial P_0}{\partial q} \tag{59}$$

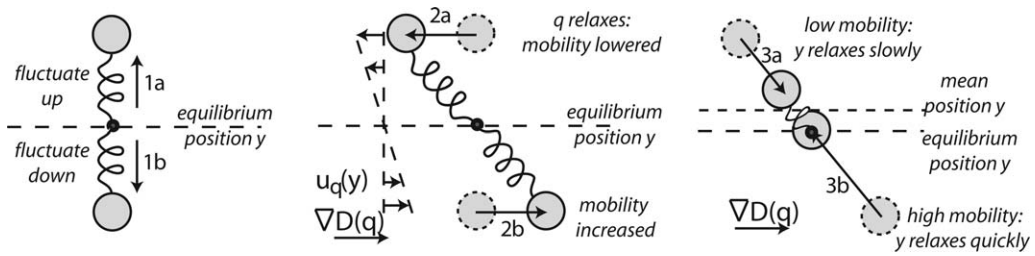

Figure 2. Fundamental physical mechanism for differential relaxation.

(a) The solute makes a diffusive step either up (1a) or down (1b), with equal probability, leading to no net change in the ensemble-averaged position of the particles. (b) The solute "configuration" is driven by a local "configuration advection," that is different for up (2a) and down (2b) steps. The solute configuration rapidly equilibrates to a new quasisteady mean configuration. The ensemble-averaged center of mass continues to remain unchanged. (c) The solute molecules relax back to the center. However, as the mean diffusivity (or, equivalently, mobility) of the solute is lower for the "up" step (3a) than for the "down" step (3b), the latter relaxes to the center more quickly. The slower relaxation from above causes the mean position to rise, eventually establishing cross-stream concentration gradients over the relaxation time scale.

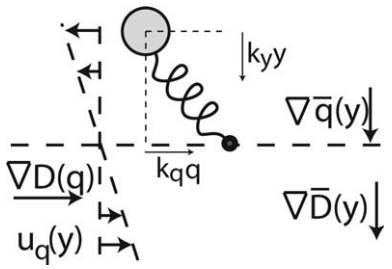

Figure 3. Definition sketch for the simplest model system for differential relaxation.

A solute whose position y and configuration q are both confined by harmonic springs. The "configuration advection" $u_q(y)$ is spatially dependent and nonconservative, and diffusivity $D_{yy}(q)$ depends on configuration.

$$= \int_0^t \int \int_{-\infty}^{\infty} \left(y' \frac{\partial P_0(q', y', t', 0, 0, 0)}{\partial q'} \right) P_0(q, y, t; q', y', t') dq' dy' dt' \tag{60}$$

The term in parenthesis reflects "scattering" at time t'—here due to position-dependent advection—and the second free propagator P_0 takes the "scattered" probability at time t' and propagates it forward to time t.

As shown in Appendix B, the $\mathcal{O}(\alpha)$ probability is

$$P_\alpha(q, y, t) = -qyf(q, 0, t, 0)g(y, 0, t, 0)H_\alpha(t) \tag{61}$$

where

$$H_\alpha(t) = \frac{\frac{\tau}{1+\tau} - \frac{\tau e^{-2t/\tau}}{\tau - 1} + \frac{2\tau e^{-\frac{\tau+1}{\tau}t}}{\tau^2 - 1}}{(1 - e^{-2t})(1 - e^{-2t/\tau})} \tag{62}$$

At times long enough for the system to relax to steady state $(t \gg \tau)$, $P_\alpha(q, y, t)$ approaches the steady value P_α^s given in (47).

In principle $P_{\alpha\beta}$ can be computed through straightforward, but involved, Gaussian integrals. As discussed earlier for the steady solutions, $P_{\alpha\beta}$ captures processes whereby the advectively perturbed probability (αP_α) experiences a configuration-dependent relaxation involving β. From the arguments we presented above, we expect that precisely those terms give rise to the eventual accumulation of probability in the "slow-relaxation" regions. Indeed, the mean position

$$\langle y \rangle = \alpha\beta \int \int y P_{\alpha\beta} dy dq \tag{63}$$

is shown in Appendix B to be

$$\langle y \rangle = \frac{\tau^2}{\tau + 1} + \frac{\tau^2 e^{-2t/\tau}}{\tau - 1} - 2\frac{\tau e^{-\frac{1+\tau}{\tau}t}}{\tau^2 - 1} - 2\tau e^{-\frac{t}{\tau}} \tag{64}$$

The mean position $\langle y \rangle$ asymptotes to $P_{\alpha\beta}^s$ (from Eq. 52), and is plotted in Figure 4. As expected from Eq. 23 the initial mean drift $d\langle y \rangle / dt|_{t=0}$, is identically zero. Despite the nonzero gradient in the average cross-stream diffusivity

$$\left. \frac{\partial \langle D_{yy}(q) \rangle}{\partial y} \right|_{t=0} \neq 0 \tag{65}$$

the mean position does not change before the concentration profile has a chance to relax. Had there been a true cross-stream drift velocity due to cross-stream diffusivity gradients, it would have been evident even at $t = 0$.

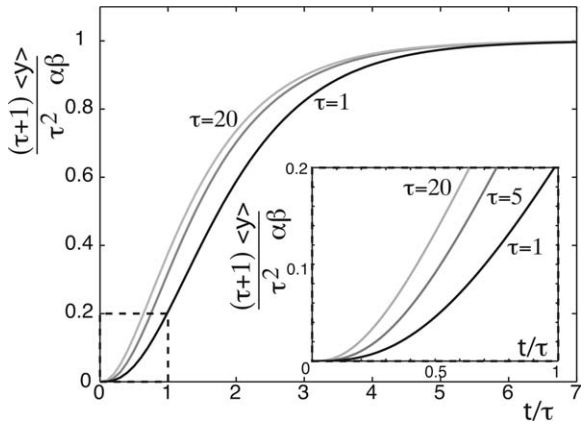

Figure 4. The mean position $\langle y \rangle$ as a function of time for the doubly harmonic solute (from Eq. 64).

Note that the slope $d\langle y \rangle / dt$ is zero at $t = 0$, as the mean position builds up via differential relaxation, rather than a directed cross-stream migration. Over the characteristic relaxation time, the mean position saturates to the value given by (52).

Singly harmonic well, between two walls

We now turn to a second example (Figure 5), which is more cumbersome mathematically, but is a closer analogy to the simplest system we described earlier, and which most clearly demonstrates the mechanism by which concentration accumulates. In particular, we consider a particle whose position Y is confined by two hard walls (i.e., no forces except to confine it between $\pm h$), whereas "configurations" Q are confined within a harmonic potential centered at $Q = 0$, as shown in Figure 5. We take the configuration-dependent diffusivity $D_{yy}(Q)$ to be given by (30), and the advective velocity

$$u_q = -U_0 \sin(\pi Y / 2h) \tag{66}$$

to simplify an image treatment, as will soon be apparent. This gives a Smoluchowski equation

$$\frac{\partial P}{\partial T} = \frac{\partial}{\partial Q} \left(D_0 \frac{\partial P}{\partial Q} + U_0 \sin \frac{\pi Y}{2h} P + D_0 \frac{Q}{L_q^2} P \right) \tag{67}$$

$$+ D_0 (1 + \epsilon Q) \frac{\partial^2 P}{\partial Y^2} \tag{68}$$

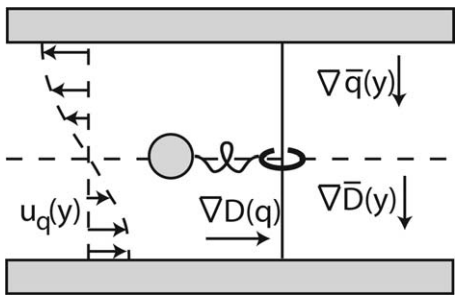

Figure 5. Definition sketch for a solute whose configuration q is harmonically confined, but which undergoes free diffusion between hard walls at $y = \pm h$.

The configuration advection $u_q(y)$ is taken to be sinusoidal, as periodic extensions of the system can be added, and walls treated with images (fig. 6).

where capital variables are dimensional. To nondimensionalize, we scale Q by typical Q-excursions from the center of the well, L_q, Y by the channel height h, and time T by the Q-relaxation time back to the center of the well L_q^2/D_0, to obtain the nondimensionalized equation

$$\frac{\partial P}{\partial t} = P_{qq} + (qP)_q + \alpha \sin\frac{\pi y}{2} P_q + \Lambda(1+\beta q) P_{yy} \tag{69}$$

where

$$\alpha = \frac{U_0 L_q}{D_0} \ll 1 \tag{70}$$

$$\beta = \epsilon L_q \ll 1 \tag{71}$$

$$\Lambda = \frac{\tau_q}{\tau_y} = \frac{L_q^2}{h^2} \ll 1 \tag{72}$$

Here, unlike the doubly periodic well, we must impose boundary conditions. Imposing a no-flux condition at the walls gives

$$D_{yy}(q) \frac{\partial P(q,y,t)}{\partial y}\Big|_{y=\pm 1} = 0 \tag{73}$$

It is straightforward to find the steady solution perturbatively, posing a regular expansion

$$P^s(q,y) = P_0^s + \alpha P_\alpha^s + \alpha\beta P_{\alpha\beta}^s \tag{74}$$

and finding

$$P_0^s(q,y) = \frac{e^{-q^2/2}}{2\sqrt{2\pi}} \tag{75}$$

$$P_\alpha^s(q,y) = -\sqrt{\frac{2}{\pi}} \frac{e^{-q^2/2} q \sin(\pi y/2)}{4+\Lambda\pi^2} \tag{76}$$

$$P_{\alpha\beta}(q,y) = \frac{2e^{-q^2/2}(8+\Lambda\pi^2 q^2)\sin(\pi y/2)}{(32+12\Lambda\pi^2+\Lambda^2\pi^4)\sqrt{2\pi}} \tag{77}$$

whereas both P_β^s and $P_{\beta\alpha}^s$ are zero.

The average position can likewise be found from P_s

$$\langle y^s \rangle = \frac{16\alpha\beta}{\pi^2(4+\Lambda\pi^2)} \tag{78}$$

in steady state. In the limit $\Lambda \ll 1$ (configurational relaxation occurring much more quickly than positional), the mean position is given by

$$\langle y^s \rangle_{\Lambda\to 0} = \frac{4\alpha\beta}{\pi^2} \tag{79}$$

As with the doubly harmonic case, the shift in the mean position occurs because the position-dependent "configurational" advection (α) drives nonuniform configurations, which then relax in an anisotropic way due to the configuration-dependent positional diffusivity (β). The steady-state nature of the solution (Eq. 74) implies that relaxation has already occurred. Irrespective, the steady solution inherently encodes the order of the processes that gives rise to cross-stream gradient formation: (1) solute molecules move diffusively (P_0); (2) a local "configurational" equilibrium is achieved (αP_α), which gives rise to a spatially inhomogeneous average mobility/diffusivity; and (3) relaxation back to the center proceeds at different rates for solute in different locations ($\alpha\beta P_{\alpha\beta}$). Solute in regions with relatively slow mobility take more time to relax than those in regions with relatively high mobility. As there is no difference (to first order) in solute flux into regions of high or low average mobility, the fact that it takes longer for the slow solute to relax means solute will gradually and generally accumulate there.

This dynamic picture is confirmed by explicitly solving for the dynamics of the system perturbatively, treating the terms proportional to α and β as weak source terms. Doing so clarifies the physical mechanism by which the concentration gradients arise. The no-flux boundaries at $y=\pm 1$ can be naturally enforced using the method of images, whereby the walls are replaced by introducing "image" particles at $\{\pm 2, \pm 4, \pm 6, \ldots\}$, as in Figure 6. All solute particles—both the true solute as well as all images—obey the same convection–diffusion equation (69), as we have chosen the advective term to be periodic. We can thus simply solve for a single particle that starts at the origin $y_0=0$, and evolves in an infinite and unbounded system—$P_\infty(q,y,t)$—from which the image system for a particle starting at $y=2j$ can be obtained by shifting the origin to $P_\infty(q,y-2j,t)$. The solution to the bounded system, then, is given by

$$P(q,y,t) = \sum_{j=-\infty}^{\infty} P_\infty(q,y-2j,t) \tag{80}$$

We thus need only to solve for the unbounded system, which obeys

$$\mathcal{L}_0 P_\infty = \alpha \sin\left(\frac{\pi y}{2}\right) \frac{\partial P_\infty}{\partial q} + \Lambda\beta q \frac{\partial^2 P_\infty}{\partial y^2} \tag{81}$$

where

$$\mathcal{L}_0 P = \frac{\partial P}{\partial t} - \frac{\partial^2 P}{\partial q^2} - \frac{\partial}{\partial q}(qP) - \Lambda \frac{\partial^2 P}{\partial y^2} \tag{82}$$

subject to the initial condition

$$P_\infty(q,y,0) = \delta(q)\delta(y) \tag{83}$$

The unperturbed propagator, which obeys $\mathcal{L}_0 P_\infty^0 = 0$ and reflects the probability that a particle starting at q', y' at time t' is found at q, y at time t is given by

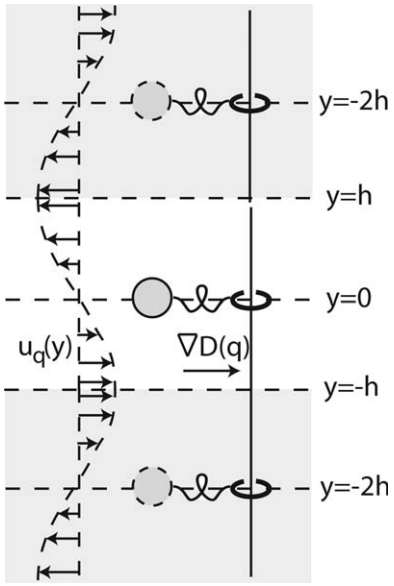

Figure 6. The walls at $y=\pm h$ in Figure 5 can be treated using images.

An infinite series of image particles, located at $y=\pm 2jh$, with integer values of j, diffuse in an infinite system.

$$P^0_\infty(q,y,t;q',y',t')=f_0(q,q',t,t')g_0(y,y',t,t') \tag{84}$$

where

$$f_0(q,q',t,t')=\frac{e^{-\frac{(q-q'h)^2}{2(1-h^2)}}}{\sqrt{2\pi(1-h^2)}} \tag{85}$$

$$g_0(y,y',t,t')=\frac{e^{-\frac{(y-y')^2}{4\Lambda(t-t')}}}{2\sqrt{\pi\Lambda(t-t')}} \tag{86}$$

and

$$h=e^{-(t-t')} \tag{87}$$

The approach is entirely analogous to that given for the doubly harmonic case: the right-hand side terms are treated perturbatively as distributions of sources and sinks of probability that continuously arise and subsequently evolve via the free-particle propagator $P^0_\infty(q,y,t;q',y',t')$. Details of the solution are given in Appendix C. As expected, the first nonzero mean drift arises due to $P_{\alpha\beta}$—reflecting nonuniform configuration "advection," followed by anisotropic relaxation. The mean drift, computed in Appendix C, is shown in Figure 7.

Thus, the dynamic mechanism in Figure 2 is responsible for these steady-state concentration gradients: (1) the particle fluctuates up or down, and the position-dependent advection (proportional to α) changes the mean configuration q; (2) the configuration difference "above" and "below" give rise to different mean diffusivities/mobilities "above" and "below"; (3) the difference in mean mobility/diffusivity "above" and "below" cause relaxation from the two sides to occur at different rates. Slower relaxation on the side with lower average diffusivity gives rise to a gradual accumulation of solute there.

Notably, no cross-stream migratory drift velocity is driven by gradients in average diffusivity. At times much shorter than the positional relaxation time ($T \ll 1$, or equivalently $t \ll h^2/D_0$), the cross-stream velocity is exponentially small (Figure 7), since at small times

$$\left.\frac{\langle y\rangle}{\langle y\rangle_s}\right|_{T\ll 1} \sim \sqrt{T}\exp\left(\frac{-1}{4T}\right) \tag{88}$$

meaning

$$\left.\frac{d\langle y\rangle}{dT}\right|_{T\ll 1} \sim \frac{1}{T^{3/2}}\exp\left(\frac{-1}{4T}\right) \tag{89}$$

On these short time scales, the exponentially small shift in $\langle y\rangle$ reflects the exponentially small probability that a particle starting at $y=0$ has diffused to the wall $y=h$. Correspondingly, the probability that any such particles have started to "relax" is exponentially small. As all shifts in $\langle y\rangle$ arise purely due to asymmetric relaxation, it is only over the positional relaxation time scales that $\langle y\rangle$ changes appreciably.

Finally, we connect this calculation back to the original observations motivating this work: polymers or rods carried with a pressure-driven (Poiseuille) flow along a channel. In these systems, the channel center is generally a location of zero shear rate, giving the most randomly aligned rods or unstretched polymers. As this is the highest-mobility state, migration will generally occur away from channel centers. The examples above, for which $\langle D\rangle(y)$ increased monotonically with y, would correspond, for example, to the upper half of a channel in these flowing systems, such that polymer/rod accumulation at $y>0$ corresponds to migration away from the channel centerline. Alternately, one could use, for example, a magnetic field to externally align rods at some angle relative to the channel. For example, shear might rotate the rods above the centerplane to be more aligned with the flow, whereas it would rotate those rods below the centerline to be more perpendicular to the flow. In this case, the diffusivity would decrease monotonically in the $+y$-direction, and anisotropic relaxation would drive a net accumulation above the centerline.

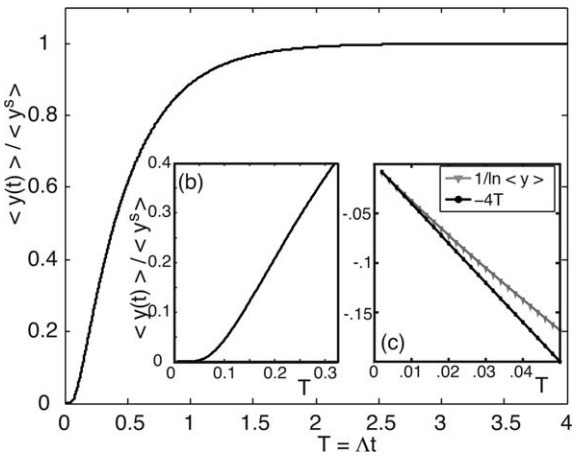

Figure 7. (a) The ensemble-averaged position $\langle y\rangle$ vs. time, for a particle of the configurationally harmonic, diffusive particle of Figure 5.

(b) There is no drift for very small times: the only mechanism by which $\langle y\rangle$ changes is via differential relaxation, and (c) at short times there is an exponentially small probability ($\sim e^{-1/4T}$ or $e^{-h^2/4D_0t}$) that a particle will encounter the wall and relax. Over the positional relaxation time scale h^2/D_0, however, the average position does indeed change and asymptote to that given by (79).

Two-state system

The above two examples involved a "continuous" degree of freedom (e.g., rod orientation). We now illustrate with a third model system which can adopt a discrete set of "configurations" (e.g., a protein that can exist in folded or unfolded states, fig. 8.) For simplicity, we will focus on a solute with two states, confined by rigid walls at $Y=\pm L$, and will denote the probability of being in either state as $a(y,t)$ or $b(y,t)$. The two states have different diffusivities

$$D_a=(1-\epsilon)D_0 \tag{90}$$

$$D_b=(1+\epsilon)D_0 \tag{91}$$

These discrete, state-dependent diffusivities are analogous to a diffusivity that depends on a configuration described by a continuous variable q. For simplicity, we will consider transitions between solute states to occur with equal forward and backward rate constants $K_{a\to b}=K_{b\to a}\equiv K$. The internal degrees of freedom must be driven in a nonconservative, position-dependent way—here an additional, externally triggered $b\to a$ transition (e.g., laser light with an intensity gradient that unfolds a macromolecule). Specifically, we choose this nonconservative transition to have sinusoidal spatial dependence, $\alpha K\sin(\pi Y/2L)$, to allow image systems as in Figure 6. The evolution of the system is then described by

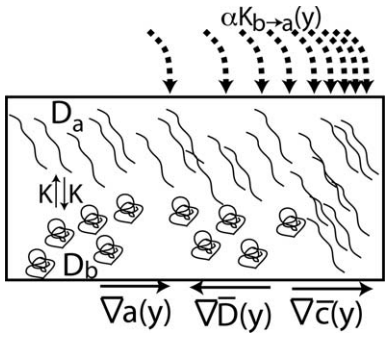

Figure 8. Definition sketch for a two-state system, which demonstrates differential relaxation for a solute with discrete configurations.

A macromolecule can be folded (b) or unfolded (a), with (high and low) diffusivities D_b and D_a, respectively. In equilibrium, the two states are equally likely, with identical forward and reverse rate constants K. Particle unfolding is triggered by an external, spatially varying mechanism. Particles are equally likely to diffuse to the right as to the left; once doing so, those to the right have a higher chance of unfolding than those to the left. When these particles relax to steady state, then, those to the right relax more slowly than those to the left, giving rise to a net accumulation of particles in the slow-average-diffusion region.

$$\frac{\partial a}{\partial T}=D_a\frac{\partial^2 a}{\partial Y^2}+K(b-a)+\alpha K\sin\left(\frac{\pi Y}{2L}\right)b \tag{92}$$

$$\frac{\partial b}{\partial T}=D_b\frac{\partial^2 b}{\partial Y^2}-K(b-a)-\alpha K\sin\left(\frac{\pi Y}{2L}\right)b \tag{93}$$

Note that analog of the "position-dependent configuration advection" in the systems with continuous internal degrees of freedom q is here given by a position-dependent transition rate constant $\alpha K\sin(\pi Y/2L)$.

First, we demonstrate the absence of any net drift in an unbounded system. Adding the equations for both states, multiplying by Y and integrating over Y gives an evolution equation for the mean position $\langle Y\rangle$

$$\int Y(\dot{a}+\dot{b})dY\equiv\dot{\bar{Y}}=D_a\int Ya_{YY}dy+D_b\int Yb_{YY}dY \tag{94}$$

Each of these terms can be integrated by parts twice, precisely as in (24), to give

$$\dot{\bar{Y}}=D_a\{a(L)-a(-L)\}+D_b\{b(L)-b(-L)\} \tag{95}$$

In an infinite system, where $L\to\infty,\dot{\bar{Y}}=0$ at any finite time. Finite systems, however, show anisotropic relaxation $b(L)\neq b(-L)$.

We can, as well, find the approximate steady-state distribution, in the limit where gradients in the Y-direction are gentle (a condition that can be checked *a posteriori*). In such a case, at any given position the two populations reach a local nonequilibrium steady state, in which the equilibrium and driven transitions balance

$$K(b_s-a_s)+\alpha K\sin\left(\frac{\pi y}{2L}\right)b_s\approx 0 \tag{96}$$

This gives a local relationship between the two populations

$$b_s(Y)=\frac{1}{1+\alpha\sin\left(\frac{\pi Y}{2L}\right)}a_s(Y) \tag{97}$$

For the populations to be in true steady state, there can be no net flux of solute in the y-direction

$$D_a\frac{\partial a_s}{\partial Y}+D_b\frac{\partial b_s}{\partial Y}=0 \tag{98}$$

which implies

$$D_a a_s(Y)+D_b b_s(Y)=C_0 \tag{99}$$

Equations 97 and 99 give the steady-state concentration of each state

$$a_s(Y)=C_0\frac{1+\alpha\sin\left(\frac{\pi Y}{2L}\right)}{D_a\left(1+\alpha\sin\left(\frac{\pi Y}{2L}\right)\right)+D_b} \tag{100}$$

$$b_s(Y)=C_0\frac{1}{D_a\left(1+\alpha\sin\left(\frac{\pi Y}{2L}\right)\right)+D_b} \tag{101}$$

and thus, the total solute concentration

$$c_s(Y)=a_s(Y)+b_s(Y) \tag{102}$$

$$=C_0\frac{2+\alpha\sin\left(\frac{\pi Y}{2L}\right)}{D_a\left(1+\alpha\sin\left(\frac{\pi Y}{2L}\right)\right)+D_b} \tag{103}$$

Once again, one sees that three ingredients must exist for a steady-state non-Boltzmann profile. First, the diffusivity must depend on conformation: if $D_a=D_b$, then (103) gives a constant concentration. Second, the conformation must be driven in a position-dependent, nonconservative way (here with an additional $b\to a$ transition that varies via $\alpha K\sin\left(\frac{\pi Y}{2L}\right)$). If $\alpha=0$, then again 103 gives a constant concentration. Finally, the concentration field must be able to relax to steady state—the steady argument given here implicitly assumes that steady state has somehow been reached, which can only occur when particle positions have had time to relax. As we showed earlier, in the absence of relaxation (e.g., in systems with no confining force), there would be identically zero drift in this system.

The mean position can be found in the $\epsilon\ll 1$ and $\alpha\ll 1$ limits by Taylor expanding (103) to yield

$$c_s\sim\frac{C_0}{D_0}+\alpha\epsilon\frac{C_0}{D_0}\frac{\sin\left(\frac{\pi Y}{2L}\right)}{2} \tag{104}$$

from which it is apparent that $C_0=D_0/2$. Next, we find the mean steady position via

$$\langle Y^s\rangle=\int_{-1}^{1}Yc_s(Y)dY=\frac{2\alpha\epsilon}{\pi^2}L \tag{105}$$

It will prove convenient to switch to "concentration" and "difference" variables

$$c=b+a \tag{106}$$

$$d=b-a \tag{107}$$

to solve for the dynamics as well as steady-state distributions. Using these variables, the governing equations become

$$\frac{\partial c}{\partial T}=D_0\frac{\partial^2 c}{\partial Y^2}+\epsilon D_0\frac{\partial^2 d}{\partial Y^2} \tag{108}$$

$$\frac{\partial d}{\partial T}=D_0\frac{\partial^2 d}{\partial Y^2}-2Kd+\epsilon D_0\frac{\partial^2 c}{\partial Y^2}-\alpha K\sin\left(\frac{\pi Y}{2L}\right)(c+d) \tag{109}$$

Nondimensionalizing time by the configurational relaxation time k^{-1} and distance by L, these become

$$\dot{c} = \Lambda\left(\frac{\partial^2 c}{\partial y^2} + \epsilon\frac{\partial^2 d}{\partial y^2}\right) \tag{110}$$

$$\dot{d} = \Lambda(d_{yy} + \epsilon c_{yy}) - 2d - \alpha \sin\left(\frac{\pi y}{2}\right)(c+d) \tag{111}$$

where

$$\Lambda = \frac{D_0}{KL^2} \ll 1 \tag{112}$$

is the ratio of the configurational relaxation time (K^{-1}) to the positional relaxation time scale (L^2/D_0), and is therefore small, and α relates the strength of "configuration advection" to the standard reaction rate.

Power series expansions give approximate steady-state distributions, with

$$d_s \sim \alpha d_\alpha^s = -\frac{2\alpha}{8+\pi^2\Lambda}\sin\left(\frac{\pi y}{2}\right) \tag{113}$$

$$c_s \sim \alpha\epsilon c_{\alpha\epsilon}^s = \frac{2\alpha\epsilon}{8+\pi^2\Lambda}\sin\left(\frac{\pi y}{2}\right) \tag{114}$$

with all other components up to $\mathcal{O}(\alpha\epsilon)$ being identically zero. The mean position

$$\langle Y^s\rangle = L\langle y^s\rangle = \frac{8}{\pi^2}\frac{2L}{8+\pi^2\Lambda}\alpha\epsilon \to \frac{2\alpha\epsilon}{\pi^2}L \tag{115}$$

reproduces (105) in the long-wavelength limit ($\Lambda \ll 1$), where positional relaxation is much slower than configurational relaxation.

The dynamics, derived in Appendix D, are essentially identical to those in Figure 7.

Suspension profiles under solute or temperature gradients

We finally turn to systems with imposed external gradients, with thermal and solute gradients as examples. Particles are known to move thermophoretically along local temperature gradients[28,29] or diffusiophoretically in solute gradients,[30,31] which naturally drive concentration gradients. Such phoretic motions are generally described by phoretic mobilities—for example, the diffusiophoretic mobility $D_P(c)$ is given by

$$U_P = D_P(c)\frac{\partial c}{\partial y} \tag{116}$$

where $\frac{\partial c}{\partial y}$ is the local solute concentration gradient that would exist in the absence of the colloid. In addition to this phoretic drift, however, such suspensions will also establish concentration gradients due to asymmetric relaxation, analogous to the systems described earlier, whenever the diffusivity depends on temperature or solute concentration.

Such suspensions exhibit the three ingredients required for differential relaxation. (1) The diffusivity of a suspended particle does not depend explicitly on position y, but rather on a degree of freedom, whether temperature T or solute concentration c. Although the temperature-dependence of diffusivity is obvious, solute dependence is more subtle. For example, the diffusivity of a charged particle depends on the local ionic strength via the electroviscous effect.[32,33] (2) The degree of freedom (T or c) is forced to be spatially inhomogeneous in a nonconservative way, as free energy must be irreversibly supplied to maintain heat or solute fluxes. (3) Any finite system presents a mechanism for concentration profiles to relax to steady state. One should, therefore, expect steady-state concentration gradients to be established due to the differential relaxation mechanism we have been discussing, in addition to any gradients that are established due to a true thermophoretic or diffusiophoretic drift.

As before, we denote the spatial co-ordinate by y and the local degree of freedom (e.g., the local temperature T or solute concentration c that would exist in the absence of the particle) by q. For clarity, we will consider q to be given by the solute concentration c, and denote the probability that a particle is located at y and surrounded by a concentration c that would exist in the absence of the particle by $P(c,y,t)$. We assume Fickian diffusion for the particles and the solute, and the particles to move with a diffusiophretic velocity given by Eq. 116. The evolution equation for $P(c,y,t)$ is given by

$$\frac{\partial P}{\partial t} = \frac{\partial}{\partial y}\left(D(c)\frac{\partial P}{\partial y}\right) + \frac{\partial}{\partial c}\left(D_c\frac{\partial c}{\partial y}\right) - \frac{\partial}{\partial y}\left(D_P\frac{\partial c}{\partial y}P\right) \tag{117}$$

For simplicity, we start by assuming no phoretic drift ($D_P = 0$), so that the colloidal flux

$$j_y = -D(c)\frac{\partial P(c,y,t)}{\partial y} \tag{118}$$

is purely diffusive. We also assume the solute concentration c to have an externally imposed linear gradient

$$c(y) = \frac{\partial \bar{c}}{\partial y}y \tag{119}$$

Under this simplified picture, the total particle flux is given by

$$J_y(y,t) = -\int D(c)\frac{\partial P(y,c,t)}{\partial y}dc \tag{120}$$

and must vanish in steady state, requiring

$$J_y^s = 0 = -\frac{\partial}{\partial y}\int D(c)P^s(y,c,t)dc \tag{121}$$

We define the steady probability P^s in terms of a local concentration $C^s(y)$ and a normalized probability distribution $p^s(y,c)$

$$P^s(y,c) = C^s(y)p^s(y,c) \tag{122}$$

where

$$\int p^s(y,c)dc = 1 \tag{123}$$

The steady, spatially inhomogeneous concentration C^s is then given by

$$C^s(y) = \frac{C_0}{\int p^s(y,c)D(c)dc} \equiv \frac{C_0}{\bar{D}(y)} \tag{124}$$

Even in the absence of any true phoretic drift, an inhomogeneous concentration profile thus develops in steady state.

Locally expanding $\bar{c}(y)$ and $D(c)$

$$\bar{c}(y) \approx \bar{c}_0 + \frac{\partial \bar{c}}{\partial y}(y - y_0) \tag{125}$$

$$D(c) \approx D_0(1 + \beta(c - c_0)) \tag{126}$$

gives an average diffusivity

$$\bar{D}(y) \approx D_0(1+\beta(\bar{c}-\bar{c}_0)) \tag{127}$$

$$\approx D_0\left(1+\beta\frac{\partial\bar{c}}{\partial y}(y-y_0)\right) \tag{128}$$

The steady-state particle concentration then follows from (124) as approximately

$$C^s(y)=\frac{C_0}{D_0}\left(1-\beta\frac{\partial\bar{c}}{\partial y}(y-y_0)\right) \tag{129}$$

If, conversely, a phoretic migration (Eq. 116) were included, the steady state particulate flux would be given by

$$J_y=-D(c)\frac{\partial C^s}{\partial y}+D_P\frac{\partial\bar{c}}{\partial y}C^s \tag{130}$$

which must vanish, giving

$$\frac{\partial \ln C^s}{\partial y}=\frac{D_P}{D(c)}\frac{\partial\bar{c}}{\partial y} \tag{131}$$

To compare the magnitude of these effects, we now compute the equivalent local phoretic drift velocity that would reproduce the concentration gradient arising from anisotropic relaxation. Using the local expansion of C^s for the nonphoretic system (Eq. 129) in the equation giving zero-flux for a phoretic drift (Eq. 131) gives an apparent phoretic mobility D_P^{app}

$$\frac{D_P^{\text{app}}}{D_0}\frac{\partial\bar{c}}{\partial y}=-\beta\frac{\partial\bar{c}}{\partial y}+\mathcal{O}(\beta^2) \tag{132}$$

meaning that the concentration gradients due to anisotropic relaxation are equivalent to those arising from an equivalent phoretic mobility

$$D_P^{\text{app}}=-\beta D_0\equiv-\frac{dD(c)}{dc} \tag{133}$$

The anisotropic relaxation of particle concentration fields, which we have shown to cause particle accumulation where average diffusivities are low, gives concentration gradients that are equivalent to those that would arise from a phoretic velocity down the diffusivity gradient. Diffusiophoresis and thermophoresis can occur either up or down gradients in solute[31] or temperature.[29] Anisotropic relaxation, conversely, always builds concentration in low-diffusivity regions. A more significant distinction, however, is that the particles migrating phoretically exhibit a net drift velocity ($\langle\dot{y}\rangle\neq 0$), whereas those accumulating via asymmetric relaxation experience identically zero net drift unless the concentration profiles are themselves relaxing spatially.

Discussion and Conclusions

We have here presented and discussed anisotropic relaxation as a central mechanism by which concentration (or probability) gradients form across streamlines in suspensions where no net, directed migration occurs. In particular, we have argued that such gradients form via a three-step process: (1) the solute takes diffusive steps across streamlines to regions where different configurations/internal degrees of freedom are more likely; (2) internal degrees of freedom, or configurations, quickly equilibrate to reach a new quasi-steady state whose average diffusivity and mobility are different; (3) the solute positions relax to steady state (whether bound by forces or constrained to remain within walls) with a rate determined by the mean mobility. Low-mobility states take longer to relax, so probability gradually accumulates in low-mobility regions. We have thus argued that cross-stream concentration gradients arise whenever three conditions are met: (1) the translational diffusivity depends on an internal degree of freedom, (2) internal degrees of freedom must be driven in a nonconservative, position-dependent manner, and (3) some mechanism must exist for the concentration fields in the system to relax to steady state.

In treating conservative systems with diffusivity gradients, naive algorithms that neglect the $\nabla\cdot\mathbf{D}$ drift velocity give rise to erroneous steady concentration profiles, with low concentrations in regions of low diffusivity (see, e.g., Ref. 34 for a discussion). Correct algorithms incorporate the $\nabla\cdot\mathbf{D}$ drift, for example, Ermak and McCammon's algorithm[35] introduces the drift explicitly, whereas Fixman's algorithm[36] involves a higher-order midpoint scheme which naturally incorporates the drift. Such naive algorithms, in fact, correspond directly to the (correct) dynamics of the systems we discussed earlier, where diffusivity depends on conformation, which is nonconservatively forced in a position-dependent way. In the cases, we described above, there is identically zero $\nabla\cdot\mathbf{D}$ drift, as $\mathbf{D}$ depends on configuration, rather than position. This can be seen, as well, in Ma & Graham's kinetic theory of polymers in flowing systems[6]: what appears to be a cross-stream migratory drift term $(-\nabla\cdot\mathbf{D})$, in fact, cancels the cross-stream migratory drift in the Fickian diffusion term that would otherwise exist in a truly conservative system. It seems ironic that it is actually the absence of cross-stream, $\nabla\cdot\mathbf{D}$ drift that gives rise to cross-stream gradients.

The three conditions we have outlined above are quite general, and we have discussed several example systems to highlight different realizations of the basic idea. Anisotropic relaxation does provide a mechanism for concentrating particles in certain regions of flow, and could thus in principle be used for separations. It must be remembered, however, that anisotropic relaxation, as we have been describing here, gives rise to identically zero directed drift, with gradients only forming over the timescales with which the suspension concentration profile itself relaxes. Although potentially effective, asymmetric relaxation may thus be considerably slower than other separation mechanisms.

Literature Cited

1. Squires TM, Messinger RJ, Manalis SR. Making it stick: convection, reaction and diffusion in surface-based biosensors. *Nat Biotechnol*. 2008;26(4):417–426.
2. Agarwal US, Dutta A, Mashelkar RA. Migration of macromolecules under flow—the physical origin and engineering implications. *Chem Eng Sci*. 1994;49(11):1693–1717.
3. Nitsche LC, Hinch EJ. Shear-induced lateral migration of Brownian rigid rods in parabolic channel flow. *J Fluid Mech*. 1997;332: 1–21.
4. Schiek RL, Shaqfeh ESG. Cross-streamline migration of slender Brownian fibres in plane poiseuille flow. *J Fluid Mech*. 1997;332: 23–39.
5. Jendrejack RM, Schwartz DC, de Pablo JJ, Graham MD. Shear-induced migration in flowing polymer solutions: simulation of long-chain DNA in microchannels. *J Chem Phys*. 2004;120(5):2513–2529.
6. Ma HB, Graham MD. Theory of shear-induced migration in dilute polymer solutions near solid boundaries. *Phys Fluids*. 2005;17(8): 083103.
7. Chen YL, Graham MD, de Pablo JJ, Jo K, Schwartz DC. DNA molecules in microfluidic oscillatory flow. *Macromolecules*. 2005; 38(15):6680–6687.

8. Usta OB, Ladd AJC, Butler JE. Lattice-Boltzmann simulations of the dynamics of polymer solutions in periodic and confined geometries. *J Chem Phys*. 2005;122(9):094902.
9. Khare R, Graham MD, de Pablo JJ. Cross-stream migration of flexible molecules in a nanochannel. *Phys Rev Lett*. 2006;96(22):224505.
10. Hernandez-Ortiz JP, Ma HB, Pablo JJ, Graham MD. Cross-streamline migration in confined flowing polymer solutions: theory and simulation. *Phys Fluids*. 2006;18(12):123101.
11. Usta OB, Butler JE, Ladd AJC. Flow-induced migration of polymers in dilute solution. *Phys Fluids*. 2006;18(3):031703.
12. Saintillan D, Shaqfeh ESG, Darve E. Effect of flexibility on the shear-induced migration of short-chain polymers in parabolic channel flow. *J Fluid Mech*. 2006;557:297–306.
13. Usta OB, Butler JE, Ladd AJC. Transverse migration of a confined polymer driven by an external force. *Phys Rev Lett*. 2007;98(9):098301.
14. Butler JE, Usta OB, Kekre R, Ladd AJC. Kinetic theory of a confined polymer driven by an external force and pressure-driven flow. *Phys Fluids*. 2007;19(11):113101.
15. Bird RB, Curtiss CF, Armstrong RC, Hassager O. *Dynamics of Polymeric Liquids*, 2nd ed. New York: Wiley-Interscience, 1987.
16. Purcell EM. Life at low Reynolds number. *Am J Phys*. 1977;45(1):3–11.
17. Leal LG. *Advanced Transport Phenomena: Fluid Mechanics and Convective Transport Processes*. Cambridge: Cambridge University Press, 2007.
18. Happel J, Brenner H. *Low Reynolds Number Hydrodynamics*. The Hague: Martinus Nijhoff Publishers, 1983.
19. Segre G, Silberberg A. Behaviour of macroscopic rigid spheres in Poiseuille flow. 2. Experimental results and interpretation. *J Fluid Mech*. 1962;14(1):136–157.
20. Ho BP, Leal LG. Inertial migration of rigid spheres in 2-dimensional unidirectional flows. *J Fluid Mech*. 1974;65:365–400.
21. Di Carlo D. Inertial microfluidics. *Lab Chip*. 2009;9(21):3038–3046.
22. Leighton D, Acrivos A. Measurement of shear-induced self-diffusion in concentrated suspensions of spheres. *J Fluid Mech*. 1987;177:109–131.
23. Pine DJ, Gollub JP, Brady JF, Leshansky AM. Chaos and threshold for irreversibility in sheared suspensions. *Nature*. 2005;438(7070):997–1000.
24. Barbee JH, Cokelet GR. Fahraeus effect. *Microvasc Res*. 1971;3(1):6–16.
25. Smart JR, Leighton DT. Measurement of the drift of a droplet due to the presence of a plane. *Phys Fluids*. 1991;3(1):21–28.
26. Leal LG, Hinch EJ. The rheology of a suspension of nearly spherical particles subject to Brownian rotations. *J Fluid Mech*. 1972;55:745–765.
27. Van Kampen NG. *Stochastic Processes in Physics and Chemistry*. Amsterdam: Elsevier, 2007.
28. Duhr S, Braun D. Why molecules move along a temperature gradient. *Proc Natl Acad Sci USA*. 2006;103(52):19678–19682.
29. Würger A. Thermal non-equilibrium transport in colloids. *Rep Prog Phys*. 2010;73(12):126601.
30. Anderson JL. Colloid transport by interfacial forces. *Annu Rev Fluid Mech*. 1989;21:61–99.
31. Prieve DC, Anderson JL, Ebel JP, Lowell ME. Motion of a particle generated by chemical gradients. *Part 2. Electrolytes. J Fluid Mech*. 1984;148:247–269.
32. Booth F. The electroviscous effect for suspensions of solid spherical particles. *Proc R Soc A*. 1950;203(1075):533–551.
33. Sherwood JD. The primary electroviscous effect in a suspension. *J Fluid Mech*. 1980;101:609–629.
34. Grassia PS, Hinch EJ, Nitsche LC. Computer-simulations of brownian-motion of complex-systems. *J Fluid Mech*. 1995;282:373–403.
35. Ermak DL, McCammon JA. Brownian dynamics with hydrodynamic interactions. *J Chem Phys*. 1978;69(4):1352–1360.
36. Fixman M. Simulation of polymer dynamics. *1. General theory. J Chem Phys*. 1978;69(4):1527–1537.
37. Hinch EJ. *Perturbation Methods*. Cambridge: Cambridge University Press, 1991.

Appendix A: Gaussian Integrals for $q_0 = 0$

We are interested in computing integrals of the form

$$I_n = \int_{-\infty}^{\infty} q'^n g(q,q',t,t') g(q',0,t',0) dq' \tag{A1}$$

where

$$g(q,q',t,t') = \frac{\exp\left(-\frac{(q-q'h)^2}{2\tau(1-h^2)}\right)}{\sqrt{2\pi\tau(1-h^2)}} \tag{A2}$$

and

$$h = e^{-(t-t')/\tau} \tag{A3}$$

Defining

$$h_0 = e^{-t'/\tau} \tag{A4}$$

$$h_1 = e^{-(t-t')/\tau} \tag{A5}$$

$$\delta = 1 - e^{-2t/\tau} \tag{A6}$$

$$A = \frac{\delta}{2\tau(1-h_0^2)(1-h_1^2)} \tag{A7}$$

$$B = \frac{h_1 q}{\tau(1-h_1^2)} \tag{A8}$$

$$C = \exp\left(-\frac{q^2}{2\tau(1-h_1^2)}\right) \tag{A9}$$

we must compute

$$I_n = \frac{C}{2\pi\tau\sqrt{(1-h_0^2)(1-h_1^2)}} \int_{-\infty}^{\infty} q'^n e^{-Aq'^2+Bq'} dq' \tag{A10}$$

We then scale $u = \sqrt{A}q$ and complete the square, giving

$$I_n = \frac{g(q,0,t,0)}{\sqrt{\pi}A^{n/2}} \int_{-\infty}^{\infty} \left(v + \frac{B}{2\sqrt{A}}\right)^n \exp\left(-v^2\right) dv \tag{A11}$$

where we have used the simplifications

$$Ce^{B^2/(4A)} = \exp\left(-\frac{q^2}{2\tau\delta}\right) \tag{A12}$$

$$A^{(n+1)/2}\sqrt{(1-h_0^2)(1-h_1^2)} = \frac{A^{n/2}\delta^{1/2}}{\sqrt{2\tau}} \tag{A13}$$

and

$$\frac{B}{2\sqrt{A}} = h_1 q \left(\frac{(1-h_0^2)}{2\tau\delta(1-h_1^2)}\right)^{1/2} \tag{A14}$$

The polynomial must then be expanded, and the integrals can be done easily

$$\int_{-\infty}^{\infty} v^n e^{-v^2} dv = \sqrt{\pi} V_n \tag{A15}$$

where $V_0 = 1, V_2 = 1/2, V_4 = 3/4, V_6 = 15/8, V_8 = 105/16$ and so on, giving

$$I_0 = \frac{e^{-\frac{q^2}{2\delta\tau}}}{\sqrt{2\pi\tau}\delta^{1/2}} \equiv g(q,0,t,0) \tag{A16}$$

$$I_1 = g(q,0,t,0)\frac{(1-h_0^2)h_1}{\delta} q \tag{A17}$$

$$I_2 = \left(\frac{\tau(1-h_0^2)(1-h_1^2)}{\delta} + \frac{(1-h_0^2)^2}{\delta^2} h_1^2 q^2\right) g(q,0,t,0) \tag{A18}$$

Appendix B: Doubly Harmonic Well—Development

Here, we compute the dynamics of the particle in the doubly harmonic well, shown in figs. 3-4, which obeys the Smoluchowski equation

$$\mathcal{L}_0 P_\infty = \alpha \sin\left(\frac{\pi y}{2}\right)\frac{\partial P_\infty}{\partial q} + \Lambda\beta q \frac{\partial^2 P_\infty}{\partial y^2} \tag{B1}$$

doubly harmonic well. We assume the particle to be located at the origin at time $t=0$, meaning that it has a probability $P_0(q', y', t', 0, 0, 0)$ of being located at $\{q', y'\}$ at a later time t'. At each time t', the "advective" perturbation introduces a distribution of weak sources and sinks, $\alpha y' \partial P_0/\partial q'$, which then propagate in time via $P_0(q, y, t; q', y', t')$ to contribute to the resulting probability of being at $\{q, y\}$ at time t. The full advective contribution is found by integrating over all times from zero to t

$$P_\alpha(q, y, t) = \mathcal{L}_0^{-1} y \frac{\partial P_0}{\partial q} \tag{B2}$$

$$= \int_0^t \int\int \left(y' \frac{\partial P_0(q', y', t', 0, 0, 0)}{\partial q'} \right) P_0(q, y, t; q', y', t') dq' dy' dt' \tag{B3}$$

The term in parenthesis reflects "scattering" at time t', and the second free propagator P_0 takes the "scattered" probability at time t' and propagates it forward to time t. This integral can be written

$$P_\alpha(q, y, t) = \int_0^t F_\alpha(q, t, t') G_\alpha(q, t, t') dt' \tag{B4}$$

where

$$F_\alpha(q, t, t') = \int_{-\infty}^{\infty} \frac{\partial f(q', 0, t', 0)}{\partial q'} f(q, q', t, t') dq' \tag{B5}$$

$$= \int_{-\infty}^{\infty} -\frac{q' f(q', 0, t', 0)}{(1 - e^{-2t'})} f(q, q', t, t') dq' \tag{B6}$$

$$= -\frac{q f(q, 0, t, 0) e^{-(t-t')}}{\delta} \tag{B7}$$

$$G_\alpha(y, t, t') = \int_{-\infty}^{\infty} y' g(y', 0, t', 0) g(y, y', t, t') dy' \tag{B8}$$

$$= y g(y, 0, t, 0) \frac{e^{-(t-t')/\tau}(1 - e^{-2t'/\tau})}{\delta_\tau} \tag{B9}$$

where f and g are given by Eqs. 57 and 58 and where

$$\delta = 1 - e^{-2t} \tag{B10}$$

$$\delta_\tau = 1 - e^{-2t/\tau} \tag{B11}$$

Formulae for the Gaussian integrals are given in Appendix A. The $\mathcal{O}(\alpha)$ probability is then given by

$$P_\alpha(q, y, t) = -\frac{q y f(q, 0, t, 0) g(y, 0, t, 0)}{\delta \delta_\tau} \tag{B12}$$

$$\times \int_0^t e^{-\frac{(t-t')}{\tau}} (1 - e^{-\frac{2t'}{\tau}}) e^{-(t-t')} dt' \tag{B13}$$

which can be integrated directly to give

$$P_\alpha(q, y, t) = -q y f(q, 0, t, 0) g(y, 0, t, 0) H_\alpha(t) \tag{B14}$$

where

$$H_\alpha(t) = \frac{1}{\delta \delta_\tau}\left(\frac{\tau}{1+\tau} - \frac{\tau e^{-2t/\tau}}{\tau - 1} + \frac{2\tau e^{-\frac{\tau+1}{\tau}t}}{\tau^2 - 1} \right) \tag{B15}$$

Next, we compute $P_{\alpha\beta}$, the asymmetric relaxation of these perturbed configurations

$$P_{\alpha\beta}(q, y, t) = \mathcal{L}_0^{-1}\left(q \frac{\partial^2 P_\alpha}{\partial y^2} + \frac{q}{\tau}\frac{\partial (y P_\alpha)}{\partial y} \right) \tag{B16}$$

$$= -\int_0^t H_\alpha(t') F_{\alpha\beta} G_{\alpha\beta} dt' \tag{B17}$$

where

$$F_{\alpha\beta} = \int q'^2 f(q, q', t, t') f(q', 0, t', 0) dq' \tag{B18}$$

$$G_{\alpha\beta} = \int g(y, y', t, t') \left(\frac{\partial^2}{\partial y'^2}(y' g(y', 0, t', 0)) \right. \tag{B19}$$

$$\left. + \frac{1}{\tau}\frac{\partial}{\partial y'}\left(y'^2 g(y', 0, t', 0)\right)\right) dy' \tag{B20}$$

Computation of these integrals is tedious but straightforward. Rather than presenting all details, we compute the time dependence of the mean position

$$\langle y(t) \rangle = \alpha\beta \int\int y P_{\alpha\beta} dy dq \tag{B21}$$

$$= -\alpha\beta \int_0^t H_\alpha(t') \left(\int F_{\alpha\beta} dq \int y G_{\alpha\beta} dy \right) dt' \tag{B22}$$

and start with the integrals over q and y

$$\int F_{\alpha\beta} dq = \int q'^2 f(q', 0, t', 0) dq' \tag{B23}$$

$$= 1 - h_0^2 \tag{B24}$$

and

$$\int y G_{\alpha\beta} dy = e^{-\frac{(t-t')}{\tau}} \int y' \left(\frac{\partial^2 (y' g(y', 0, t', 0))}{\partial y'^2} \right. \tag{B25}$$

$$\left. + \frac{1}{\tau}\frac{\partial (y'^2 g(y', 0, t', 0))}{\partial y'} \right) dy' \tag{B26}$$

as

$$\int y g(y, y', t, t') dy = y' e^{-(t-t')/\tau} \tag{B27}$$

On integrating B26 by parts, the first term vanishes to leave

$$\int y G_{\alpha\beta} dy = -\frac{e^{-\frac{(t-t')}{\tau}}}{\tau} \int y'^2 g(y', 0, t', 0) dy' \tag{B28}$$

$$= -e^{-\frac{(t-t')}{\tau}} (1 - h_{0\tau}^2) \tag{B29}$$

Using B24 and B29 in B22 gives an integral for the mean position

$$\langle y(t) \rangle = \alpha\beta \int_0^t H_\alpha(t') e^{-\frac{(t-t')}{\tau}} (1 - h_{0\tau}^2)(1 - h_0^2) dt' \tag{B30}$$

which can be evaluated to give Eq. 64

$$\langle y \rangle = \frac{\tau^2}{\tau + 1} + \frac{\tau^2 e^{-2t/\tau}}{\tau - 1} - 2\frac{\tau e^{-\frac{1+\tau}{\tau}t}}{\tau^2 - 1} - 2\tau e^{-\frac{t}{\tau}} \tag{B31}$$

plotted in Figure 4.

Appendix C: Singly Harmonic with Sinusoidal Advection

Here, we compute the dynamics of the solute molecule described in section, which obeys the Smoluchowski equation

$$\mathcal{L}_0 P_\infty = \alpha \sin\left(\frac{\pi y}{2}\right)\frac{\partial P_\infty}{\partial q} + \Lambda\beta q\frac{\partial^2 P_\infty}{\partial y^2} \tag{C1}$$

where

$$\mathcal{L}_0 P = \frac{\partial P}{\partial t} - \frac{\partial^2 P}{\partial q^2} - \frac{\partial}{\partial q}(qP) - \Lambda\frac{\partial^2 P}{\partial y^2} \tag{C2}$$

subject to the initial condition

$$P_\infty(q,y,0) = \delta(q)\delta(y) \tag{C3}$$

The no-flux boundaries at $y=\pm 1$ are treated using a method of images: we solve for the dynamics of a single particle in an unbounded system, then add images at $y_j = y+2j$

$$P_\infty(q,y,0) = \delta(q)\delta(y-2j) \tag{C4}$$

We will thus start by solving perturbatively for the single-particle probability in an unbounded system and will then add the corresponding images.

The unperturbed propagator, which obeys $\mathcal{L}_0 P^0_\infty = 0$ and reflects the probability that a particle starting at q', y' at time t' is found at q, y at time t is given by

$$P^0_\infty(q,y,t;q',y',t') = f_0(q,q',t,t')g_0(y,y',t,t') \tag{C5}$$

where

$$f_0(q,q',t,t') = \frac{e^{-\frac{(q-q'h)^2}{2(1-h^2)}}}{\sqrt{2\pi(1-h^2)}} \tag{C6}$$

$$g_0(y,y',t,t') = \frac{e^{-\frac{(y-y')^2}{4\Lambda(t-t')}}}{2\sqrt{\pi\Lambda(t-t')}} \tag{C7}$$

and

$$h = e^{-(t-t')} \tag{C8}$$

The leading-order, single-particle probability that satisfies the initial conditions (C4) for the jth image is then given by

$$P^j_0 = \frac{\exp\left(-\frac{q^2}{2(1-h^2)}\right)}{\sqrt{2\pi(1-h^2)}}\frac{e^{-\frac{(y-2j)^2}{4\Lambda t}}}{2\sqrt{\pi\Lambda t}} \tag{C9}$$

At $\mathcal{O}(\alpha)$, we must compute

$$P^j_\alpha = \mathcal{L}_0^{-1}\left(\sin\left(\frac{\pi y}{2}\right)\frac{\partial P^j_0}{\partial q}\right) \tag{C10}$$

which is given by

$$P_\alpha = \int_0^t F_\alpha(q,t,t')G^j_\alpha(y,t,t')dt' \tag{C11}$$

where

$$F_\alpha(q,t,t') = \int_{-\infty}^{\infty} f_0(q,q',t,t')\frac{\partial f_0(q',0,t',0)}{\partial q'}dq' \tag{C12}$$

$$G^j_\alpha(y,t,t') = \int_{-\infty}^{\infty} g_0(y,y',t,t')g^j_0(y',2j,t',0)\sin\left(\frac{\pi y'}{2}\right)dy'$$

Letting $z' = y'-2j$ and $Y_j = y-2j$, we compute $G^j_\alpha(y)$ (C13)

$$G^j_\alpha(y) = \frac{(-1)^j}{2\sqrt{\pi\Lambda t}}e^{-Y_j^2/4\Lambda t}\sin\left(\frac{\pi Y_j t'}{2t}\right)e^{-\frac{\pi^2\Lambda(t-t')t'}{4t}} \tag{C14}$$

Now, computing F_α

$$F_\alpha(q) = -\frac{\int_{-\infty}^{\infty} q' e^{-\frac{1}{2}\left(\frac{q'^2}{1-h_0^2}+\frac{(q-q'h_1)^2}{1-h_1^2}\right)}dq'}{2\pi\sqrt{(1-h_1^2)(1-h_0^2)^3}} \tag{C15}$$

$$= -\frac{qe^{-\frac{q^2}{2\delta}}}{\sqrt{2\pi\delta^3}}e^{-(t-t')} \tag{C16}$$

gives the $\mathcal{O}(\alpha)$ unbounded, single-particle probability for the jth image

$$P^j_\alpha(q,y,t) = (-1)^{j+1}\frac{qe^{-\frac{q^2}{2\delta}}e^{-\frac{Y_j^2}{4\Lambda t}}}{2\pi\sqrt{2\Lambda t\delta^3}} \tag{C17}$$

$$\times\int_0^t \sin\left(\frac{\pi Y_j t'}{2t}\right)e^{-\frac{\pi^2\Lambda(t-t')t'}{4t}-(t-t')}dt' \tag{C18}$$

Under the substitution $t' = t(1-u)$, this becomes

$$P^j_\alpha(q,y,t) = (-1)^{j+1}\frac{qe^{-\frac{q^2}{2\delta}}e^{-\frac{Y_j^2}{4\Lambda t}t}}{2\pi\sqrt{2\Lambda t\delta^3}} \tag{C19}$$

$$\times\int_0^1 \sin\frac{\pi Y_j(1-u)}{2}e^{-\frac{\pi^2 t\Lambda u(1-u)}{4}-tu}du \tag{C20}$$

In the asymptotic limit $t \gg 1$ (i.e., many q-relaxation times), the integral is exponentially dominated around $u=0$ and is thus can be approximated using Watson's lemma.[37] Expanding the integrand around $u=0$ and computing the leading-order approximation gives

$$P_\alpha(q,y,t) \approx (-1)^{j+1}\frac{qe^{-\frac{q^2}{2\delta}}e^{-\frac{Y_j^2}{4\Lambda t}t}}{2\pi\sqrt{2\Lambda t}}\sin\left(\frac{\pi Y_j}{2}\right) \tag{C21}$$

$$\times\int_0^{`\infty'}\exp\left(-t\left(\frac{\pi^2\Lambda}{4}+1\right)u\right)du \tag{C22}$$

$$\approx (-1)^{j+1}\frac{q\sqrt{2}e^{-\frac{q^2}{2}}e^{-\frac{Y_j^2}{4\Lambda t}}}{\pi\sqrt{\Lambda t}(\pi^2\Lambda+4)}\sin\left(\frac{\pi Y_j}{2}\right) \tag{C23}$$

Note we have also taken $\delta=1$, as is appropriate in the limit $t \gg 1$. Summing all images using $Y_j = y-2j$ gives

$$P_\alpha(q,y,t) \approx (-1)^{j+1}\frac{2qe^{-\frac{q^2}{2}}}{\pi\sqrt{2\Lambda t}(\pi^2\Lambda+4)} \tag{C24}$$

$$\times\sum_{j=-\infty}^{\infty} e^{-\frac{(y-2j)^2}{4\Lambda t}}\sin\left(\frac{\pi y}{2}-j\pi\right) \tag{C25}$$

which simplifies to

$$P_\alpha(q,y,t) \approx -\frac{4qe^{-q^2/2}\sin\left(\frac{\pi y}{2}\right)}{\sqrt{2\pi}(\pi^2\Lambda+4)}\sum_{j=-\infty}^{\infty}\frac{e^{-\frac{(y-2j)^2}{4\Lambda t}}}{2\sqrt{\pi\Lambda t}} \tag{C26}$$

Note that the sum itself is the free diffusion of an infinite series particles starting at $y=\pm 2j$, which in the $t\to\infty$ limit approaches 1/2

$$\sum_{j=-\infty}^{\infty} \frac{e^{-\frac{(y-2j)^2}{4\Lambda t}}}{2\sqrt{\pi\Lambda t}} \to 1/2 \tag{C27}$$

giving the long-time behavior of P_α

$$P_\alpha(q,y,t\to\infty) \to -\frac{2qe^{-q^2/2}}{\sqrt{2\pi}(\pi^2\Lambda+4)} \sin\left(\frac{\pi y}{2}\right) \tag{C28}$$

in agreement with (76).

Last, we need to compute $P_{\alpha\beta}$, to get the leading-order mean drift due to differential relaxation. We define

$$P_\alpha(q,y,t) = -\frac{4}{(\pi^2\Lambda+4)} f_\alpha(q) g_\alpha(y,t) \tag{C29}$$

where

$$f_\alpha(q) = \frac{qe^{-q^2/2}}{\sqrt{2\pi}} \tag{C30}$$

and

$$g_\alpha(y,t) = \sin\left(\frac{\pi y}{2}\right) \sum \frac{e^{-(y-2j)^2/4\Lambda t}}{2\sqrt{\pi\Lambda t}} \tag{C31}$$

The probability $P_{\alpha\beta}$ is given by

$$P_{\alpha\beta}(q,y,t) = \mathcal{L}^{-1}(\Lambda q (P_\alpha)_{yy}) \tag{C32}$$

$$= -\frac{4\Lambda}{4+\pi^2\Lambda} \int_0^t F_{\alpha\beta}(q,t,t') G_{\alpha\beta}(y,t,t') dt' \tag{C33}$$

Here

$$F_{\alpha\beta}(q,t,t') = \int_{-\infty}^{\infty} q' f_\alpha(q',t') f_0(q,q',t,t') dq' \tag{C34}$$

and

$$G_{\alpha\beta}(y,t,t') = \int_{-\infty}^{\infty} \frac{\partial^2}{\partial y'^2} (g_\alpha(y',t')) g_0(y,y',t,t') dy' \tag{C35}$$

Our central interest concerns the quantity $\langle y(t)\rangle$, which requires integrating $P_{\alpha\beta}$ over both q and y. For simplicity, we integrate over q first

$$\langle F_{\alpha\beta}\rangle = \int_{-\infty}^{\infty} F_{\alpha\beta}(q,t,t') dq \tag{C36}$$

$$= \int dq' q' f_\alpha(q',t') \int_{-\infty}^{\infty} dq f(q,q',t,t') \tag{C37}$$

$$= \int dq' q' f_\alpha(q',t') = 1 \tag{C38}$$

to give an average probability

$$\langle P_{\alpha\beta}\rangle(y,t) = -\frac{4\alpha\beta\Lambda}{4+\pi^2\Lambda} \int_0^t G_{\alpha\beta}(y,t,t') dt' \tag{C39}$$

There is no longer any "short" time, so we rescale all times by the long (relaxation) time scale Λt

$$T = \Lambda t \tag{C40}$$

To compute $G_{\alpha\beta}$ in Eq. C13, we will consider g_α from Eq. C31 to be

$$g_\alpha(y,T) = \frac{e^{-(y-2j)^2/4T + i\frac{\pi y}{2}}}{2\sqrt{\pi T}} \tag{C41}$$

and will eventually take the imaginary part. Using

$$\frac{\partial^2 g_\alpha(y',T')}{\partial y'^2} = \frac{(-1)^j e^{-\pi^2 T'/4}}{8T'^2\sqrt{\pi T'}} \left(e^{-u'^2/4T'}(u'^2 - 2T')\right) \tag{C42}$$

where $u' = y' - 2j - i\pi T'$, and evaluating Eq. C13 gives

$$G_{\alpha\beta}(y,T') = \frac{(-1)^j e^{-\pi^2 T'/4}}{8T^{5/2}\sqrt{\pi}} \left((u^2 - 2T) e^{-\frac{u^2}{4T}}\right) \tag{C43}$$

where $u = y - 2j - i\pi T'$.

To find the mean position $\langle y(t)\rangle$, we must compute

$$\langle y(t)\rangle = -\frac{4\alpha\beta}{4+\pi^2\Lambda} \int_0^T \int_{-1}^1 y G_{\alpha\beta}(y,T') dy dT' \tag{C44}$$

We compute the integral over y first

$$\int_{-1}^1 y G_\alpha(y,t') dy = \frac{e^{\frac{-\pi^2 T'}{4}}}{4\sqrt{\pi} T^{3/2}} \sum_j (-1)^j \tag{C45}$$

$$\times e^{-\frac{(2j - y + i\pi T')^2}{4t}} (y(2j + i\pi T' - y) - 2T)\Big|_{-1}^1 \tag{C46}$$

The integral over T' can then be performed to give

$$\int_0^T \int_{-1}^1 y G_\alpha(y,t') dy dT' = \tag{C47}$$

$$-\frac{ie^{-(y-2j)^2/4T}}{2\pi^{3/2}T^{1/2}} y\left((-1)^j - e^{i\pi y/2}\right)\Big|_{-1}^1 \tag{C48}$$

$$+ i\frac{e^{-\frac{\pi^2 T}{16}} e^{\frac{i\pi(y+2j)}{4}} (i\pi y - 4)}{4\pi} \mathrm{Im\,erf}\left(\frac{4j + i\pi T - 2y}{4\sqrt{T}}\right)\Big|_{-1}^1 \tag{C49}$$

The first term (C48) vanishes on summation. Finally, using C44 gives the mean position

$$\langle y(t)\rangle = \frac{4\alpha\beta}{4+\pi^2\Lambda} \frac{e^{-\frac{\pi^2 T}{16}}}{4\pi} \tag{C50}$$

$$\times \sum_j \mathrm{Re}\left[e^{\frac{i\pi(y+2j)}{4}} (i\pi y - 4) \mathrm{Im\,erf}\left(\frac{4j + i\pi T - 2y}{4\sqrt{T}}\right)\Big|_{-1}^1\right] \tag{C51}$$

which appears in Figure 7.

Appendix D: Two-State Dynamics

The equations are

$$\dot{c} = \Lambda(c_{yy} - \epsilon d_{yy}) \tag{D1}$$

$$\dot{d} = \Lambda d_{yy} - 2d - \Lambda\epsilon c_{yy} - \alpha \sin\left(\frac{\pi y}{2}\right)(c+d) \tag{D2}$$

Unperturbed propagators are

$$c_0(y,y',t,t') = \frac{e^{-(y-y')^2/4\Lambda(t-t')}}{2\sqrt{\pi\Lambda(t-t')}} \tag{D3}$$

$$d_0(y,y',t,t') = e^{-2(t-t')} \frac{e^{-(y-y')^2/4\Lambda(t-t')}}{2\sqrt{\pi\Lambda(t-t')}} \tag{D4}$$

We start with a particle at $y = 0$, equally likely in either state

$$a(y,0) = b(y,0) = \frac{\delta(y)}{2} \tag{D5}$$

or

$$c(y,0)=\delta(y) \tag{D6}$$

$$d(y,0)=0 \tag{D7}$$

So the perturbative solution is

$$c_0(y,t)=\sum_{j=-\infty}^{\infty}\frac{e^{-(y-2j)^2/4\Lambda t}}{2\sqrt{\pi\Lambda t}}\to\frac{1}{2} \tag{D8}$$

$$d_0(y,t)=0 \tag{D9}$$

To $\mathcal{O}(\alpha)$

$$c_\alpha(y,t)=0 \tag{D10}$$

$$d_\alpha(y,t)=\frac{(-1)^{j+1}}{2\sqrt{\pi\Lambda t}}\int_0^t e^{-2(t-t')-\frac{Y^2-2i\pi Y\Lambda t'+\pi^2\Lambda^2 t'(t-t')}{4\Lambda t}}dt' \tag{D11}$$

$$=\frac{(-1)^{j+1}t}{2\sqrt{\pi\Lambda t}}\int_0^1 e^{-2tu-\frac{Y^2}{4\Lambda t}-\frac{\Lambda\pi^2 tu(1-u)-2i\pi(1-u)Y}{4}}du \tag{D12}$$

where we have made the substitution $t'=t(1-u)$. In the limit $\Lambda \ll 1$ (equilibration time short compared with diffusive relaxation), the first exponential kills the integrand for $u>\mathcal{O}(1)$, whereas the second exponential varies slowly. Taylor expanding the second around $u=0$ to use Watson's lemma gives

$$d_\alpha(y,t)\approx\frac{(-1)^{j+1}te^{-\frac{Y^2}{4\Lambda t}}e^{\frac{i\pi Y}{2}}}{2\sqrt{\pi\Lambda t}}\int_0^{'\infty'}e^{-2tu}du \tag{D13}$$

$$\approx\frac{(-1)^{j+1}}{4\sqrt{\pi\Lambda t}}e^{-\frac{Y^2}{4\Lambda t}}e^{\frac{i\pi Y}{2}} \tag{D14}$$

Taking the imaginary part and summing over all images j gives

$$d_\alpha(y,t)=-\sum_{j=-\infty}^{\infty}\frac{e^{-\frac{(y-2j)^2}{2\Lambda t}}\sin\left(\frac{\pi y}{2}\right)}{4\sqrt{\pi\Lambda t}} \tag{D15}$$

which in the limit $t\to\infty$ becomes

$$d_\alpha(y,t\to\infty)\to-\frac{1}{4}\sin\left(\frac{\pi y}{2}\right) \tag{D16}$$

Finally, we compute the $\mathcal{O}(\alpha\epsilon)$ term, this corresponds to the probability that has been advected, then anisotropically relaxes

$$c_{\alpha\epsilon}=\int_0^t\int_{-\infty}^{\infty}d^\alpha_{y'y'}\frac{e^{-(y-y')^2/4\Lambda(t-t')}}{\sqrt{4\Lambda\pi(t-t')}}dy'dt' \tag{D17}$$

Using

$$d^\alpha_{y'y'}=\frac{(-1)^j(\Lambda t'(2+\Lambda\pi^2t')+2i\Lambda\pi t'Y'-Y'^2)}{16\sqrt{\pi\Lambda^5t'^5}}e^{-\frac{Y'^2}{4\Lambda t'}}e^{\frac{i\pi Y'}{2}} \tag{D18}$$

and computing

$$\langle y\rangle(t)=\alpha\epsilon\int_0^t\int_{-1}^1\int_{-1}^1 c_{\alpha\beta}(y)ydydy'dt' \tag{D19}$$

gives a result that is functionally identical to the singly harmonic drift (Figure 7). $\langle y\rangle$ is thus exponentially small at small times ($\Lambda t\ll 1$), then approaches the steady state

$$\langle y\rangle(\Lambda t\gtrsim\mathcal{O}(1))\to-\frac{2}{\pi^2}\alpha\epsilon \tag{D20}$$

as expected (e.g., from Eq. 105).

Manuscript received Oct. 8, 2013, and revision received Dec. 24, 2013.